HHS Public Access

Author manuscript

Biochem Pharmacol. Author manuscript; available in PMC 2020 November 23.

Published in final edited form as:

Biochem Pharmacol. 2019 November ; 169: 113604. doi:10.1016/j.bcp.2019.08.006.

Cystathionine-γ-lyase (CSE) deficiency increases erythropoiesis and promotes mitochondrial electron transport via the upregulation of coproporphyrinogen III oxidase and consequent stimulation of heme biosynthesis

Katalin Módis[1,2,5], **V-M. Sadagopa Ramanujam**[3], **Armita Abdollahi Govar**[2], **Ernesto Lopez**[4], **Karl E. Anderson**[3], **Rui Wang**[5,*], **Csaba Szabo**[2,6,*]

[1]Department of Surgery, University of Texas Medical Branch, Galveston, TX, USA [2]Department of Anesthesiology, University of Texas Medical Branch, Galveston, TX, USA [3]Department of Preventive Medicine and Community Health, University of Texas Medical Branch, Galveston, TX, USA [4]Center for Translational Injury Research, Department of Surgery, University of Texas Health Science Center, Houston, TX, USA [5]Department of Biology, Lakehead University, ON, Canada [6]Chair of Pharmacology, Department of Science and Medicine, University of Fribourg, Fribourg, Switzerland

Abstract

Background: Hydrogen sulfide (H_2S) is an endogenous gasotransmitter produced by mammalian cells. The current study investigated the potential role of H_2S in the regulation of heme biosynthesis using mice deficient in cystathionine gamma-lyase (CSE), one of the three major mammalian H_2S-producing enzymes.

Methods: Wild-type and global $CSE^{-/-}$ mice, as well as mitochondria prepared from their liver were used. *In vivo*, arterial and venous blood gases were measured, and survival of the mice to severe global hypoxia was monitored. *Ex vivo*, expression of various heme biosynthetic enzymes including coproporphyrinogen oxidase (CPOX) was measured, and mitochondrial function was evaluated using Extracellular Flux Analysis. Urine samples were collected to measure the oxidized porphyrinogen intermediates. The *in vivo/ex vivo* studies were complemented with mitochondrial

*Corresponding authors: Csaba Szabo: szabocsaba@aol.com, Rui Wang: rui.wang@laurentian.ca.

Authors' contributions

Conceptualization: K.M., R.W., C.S., K.E.A.
Methodology: K.M., A.A.G., V-M. R.S., E.L.
Resources: R.W., C.S., K.M., K.E.A.
Writing: C.S., R.W., K.M., E.L.
Funding: K.M., R.W., C.S., K.E.A.

Competing interests

The authors declare no conflicts of interest in relationship to this study.

Declarations

Ethics approval and consent to participate

The study was approved by the Institutional Animal Care and Use Committee at the Lakehead University and University of Texas Medical Branch in accordance with the National Institutes of Health Guide. All experiments were performed according to relevant guidelines and regulations.

Consent for publication

There is no contains about any individual person's data in any form and there is no need to obtain consent for publication.

bioenergetic studies in hepatocytes *in vitro*. Moreover, the potential effect of H_2S on the CPOX promoter was studied in cells expressing a CPOX promoter construct system.

Results: The main findings are as follows: (1) $CSE^{-/-}$ mice exhibit elevated red blood cell counts and red blood cell mean corpuscular volumes compared to wild-type mice; (2) these changes are associated with elevated plasma and liver heme levels and (3) these alterations are likely due to an induction of CPOX (the sixth enzyme involved in heme biosynthesis) in $CSE^{-/-}$ mice. (4) Based on *in vitro* promoter data the promoter activation of CPOX is directly influenced by H_2S, the product of CSE. With respect to the potential functional relevance of these findings, (5) the increased circulating red blood cell numbers do not correspond to any detectable alterations in blood gas parameters under resting conditions, (6) nor do they affect the hypoxia tolerance of the animals in an acute severe hypoxia model. However, there may be a functional interaction between the CSE system and the CPOX system in terms of mitochondrial bioenergetics: (7) $CSE^{-/-}$ hepatocytes and mitochondria isolated from them exhibit increased oxidative phosphorylation parameters, and (8) this increase is partially blunted after CPOX silencing. However, although heme is essential for the biosynthesis of mitochondrial electron chain complexes, and CPOX is required for heme biosynthesis, (9) the observed functional mitochondrial alterations are not associated with detectable changes in mitochondrial electron transport chain protein expression.

Conclusions: The CSE system regulates the expression of CPOX and consequent heme synthesis. These effects in turn, do not influence global oxygen transport parameters, but may regulate mitochondrial electron transport.

Keywords

porphyrins; gasotransmitters; oxygen transport; mitochondria; bioenergetics; circulation; red blood cells

1. Introduction

Hydrogen sulfide (H_2S) is an endogenous gasotransmitter produced by mammalian cells. It is known to regulate a variety of physiological and pathophysiological processes in health and disease. H_2S levels in the circulation are decreased in some conditions (for instance diabetes mellitus, ischemia and aging) and are increased in other conditions (for instance in many forms of local and systemic inflammation, in various forms of critical illness and in several forms of cancer) (Wang, 2012; Szabo and Papapetropoulos, 2017).

There are three principal mammalian H_2S-producing enzymes: cystathionine beta-synthase (CBS), cystathionine gamma-lyase (CSE), and 3-mercaptopyruvate sulfurtransferase (3-MST) (reviewed in Huang and Moore, 2015; Kimura, 2015; Szabo and Papapetropoulos, 2017). Mice deficient in each of these enzymes have been generated (global knockouts); these animals present with some baseline alterations, suggesting the importance of endogenously produced H_2S in the regulation of cardiovascular and neurological functions. In addition, in several disease models, mice that are deficient in H_2S-production exhibit exacerbated pathophysiological responses, underlying the protective role of endogenously produced H_2S in the regulation of various biological processes (Rose et al., 2017).

Mice deficient in CSE have been studied for at least a decade in several laboratories. In some, but not other models of CSE deficiency, mice exhibit a mild degree of hypertension (Yang et al., 2008; Ishii et al., 2010; Szijarto et al., 2018). They also demonstrate impaired endothelium-dependent relaxant responses to vasoactive agents including muscarinic agonists (Yang et al., 2008; Coletta et al., 2012; Wen et al., 2018). There may be an enhanced pro-inflammatory response in CSE-deficient mice in response to local or systemic inflammatory insults (Gaddam et al., 2016; Ahmad et al., 2016; Liu et al., 2018). Moreover, CSE-deficient mice are also prone to atherogenesis, and insulin resistance, effects that can be reversed by H_2S supplementation (Wang et al., 2009; Mani et al., 2013; Li et al., 2017; Yang et al., 2018; Guo et al., 2019; Bibli et al., 2019). However, interestingly, there are also some conditions (e.g. pancreatitis, burn injury, and obesity) where CSE deficiency was found to confer protection (Ang et al., 2013; Ahmad et al., 2017; Yang et al., 2018).

The current article reports on our findings in CSE-deficient mice showing that the mice exhibit significant hematological changes compared to the wild-type animals. When exploring the underlying mechanisms, we have identified the upregulation of coproporphyrinogen oxidase (CPOX) – a key enzyme in heme biosynthesis – in $CSE^{-/-}$ mice. Because porphyrin synthesis, catalyzed by CPOX has an important role not only in heme synthesis and erythropoiesis, but also in the production of mitochondrial electron transport chain proteins, we have explored the potential importance of CSE-regulated CPOX in two aspects of metabolism: (a) oxygen transport and global hypoxia resistance and (b) mitochondrial electron transport and cellular bioenergetics.

2. Materials and Methods

Materials:

Adenosine 5’-diphosphate (ADP) sodium salt, antimycin A, carbonyl cyanide 4-(trifluoromethoxy) phenylhydrazone (FCCP), fatty acid-free BSA, ethylene glycol-bis(2-aminoethyl ether)-N,N,N′,N′-tetraacetic acid (EGTA), HEPES solution, magnesium chloride, d-mannitol, oligomycin, potassium phosphate monobasic, pyruvate, rotenone, sodium succinate dibasic hexahydrate, and N,N,N′,N′-tetramethyl-p-phenylenediamine dihydrochloride (TMPD) were obtained from Sigma–Aldrich (St. Louis, MO, USA). For cell culture experiments, DMEM (Dulbecco’s modified Eagle’s medium), L-glutamine, nonessential amino acids, penicillin, and streptomycin were obtained from Sigma–Aldrich (St. Louis, MO, USA), and Hyclone FBS was obtained from GE Healthcare Life Sciences (Pittsburgh, PA, USA). The H_2S-donor compound sodium hydrosulfide hydrate ($NaSH{\cdot}xH_2O$) and the CSE inhibitor, DL-propargylglycine (PAG), were purchased from Sigma–Aldrich (St. Louis, MO, USA). The Pierce bicinchoninic acid protein assay kit was purchased from ThermoFisher Scientific (Waltham, MA, USA). Anti-3-MST, anti-CSE, anti-CBS, anti-glyceraldehyde 3-phosphate dehydrogenase (GAPDH), anti-rhodanese (TST), anti-CPOX, anti-Tom20, antibodies for Western blotting were obtained from Proteintech Group, Inc. (Rosemont, IL, USA), Sigma–Aldrich (St. Louis, MO, USA), or Santa Cruz Biotechnology, Inc. (Dallas, TX, USA). For High Performance Liquid Chromatography (HPLC) experiments, HPLC grade water, methanol, acetonitrile, and ACS

high purity grade hydrochloric and glacial acetic acids, and ammonium hydroxide were purchased from Fisher Chemical Co. (Houston, TX, USA).

Animals:

All animal studies were approved by the Institutional Animal Care and Use Committee at the Lakehead University and University of Texas Medical Branch in accordance with the National Institutes of Health Guide for the Care and Use of Laboratory Animals. In-house–bred male CSE-KO mice (C57BL6/129 background) (Yang et al., 2008) were kept in a controlled, air-conditioned environment with ad libitum access to food and water on a 12-hour light/dark cycle. Male mice at age 12–16 weeks were used for experimenting. Beside tissue collection, in separate experiments, mice were subjected to 5% hypoxia for a short-term survival study or urine samples were collected using metabolic cages.

Cell culture:

HepG2, an immortalized human liver cancer cell line, was purchased from ATCC (American Type Culture Collection, Manassas, VA, USA) and maintained in DMEM containing 1 g/l glucose supplemented with 10% FBS (Hyclone), 4 mmol/l glutamine, 100 IU/ml penicillin, and 100 mg/ml streptomycin at 37°C in a 5% CO_2 atmosphere. Cells were maintained throughout serial subcultures (through 8 passages).

SiRNA-mediated CSE and CPOX silencing:

SiRNA oligonucleotides were used for transient silencing of CSE and CPOX in HepG2 cells (Silencer Select Pre-designed siRNAs #s3710 for CSE, and #s3460 for CPOX, Ambion, Life Technologies, Carlsbad, CA, USA). For CSE, the following sequence was applied: 5'–3' sense, GCAUCUGAAUUUGGAUUAAtt, and 3'–5' antisense, UUAAUCCAAAUUCAGAUGCca. For CPOX, the applied sequence contained the 5'–3' sense GGAAAAGUUCUGAAGACUAtt, and 3'–5' antisense, UAGUCUUCAGAACUUUUCCtc. For negative control, commercially available, non-targeting siRNAs were used (Silencer Select Negative Control #1 siRNA, Life Technologies, Carlsbad, CA, USA). Silencing approach was conducted in 24-well XF24 V7 Seahorse plates. 10,000 cells/well were seeded into 24-well XF24 V7 Seahorse plates to reach 70–90% confluence. The following day the growth medium was replaced with Opti-Mem medium containing 10% FBS lacking antibiotics, followed by transfection with siRNA fragments (100 nM) and Lipofectamine RNAiMAX complexes as the manufacturer's protocol recommended. Control cells were transfected in parallel with non-targeting siRNA. After 72 hours, bioenergetic measurements were performed. To optimize the siRNA concentration for maximal attenuation of target enzymes, preliminary transfections were carried out for each siRNA at 10–100 nM concentration. Silencing efficiency of CSE and CPOX were confirmed by Western blot analysis.

Isolation of mouse liver mitochondria.

The left liver lobe was harvested from $CSE^{-/-}$ and wild-type mice. Mitochondria from livers were isolated by differential centrifugation as previously described (Rogers et al., 2011). Total protein was determined using the Pierce BCA Protein Assay Reagent (Thermo Fisher

Scientific, Waltham, MA, USA). Mitochondrial preparations were used for bioenergetic analysis within 1 to 3 hours after isolation.

Measurement of red blood cell parameters:

A complete blood count test related to red blood cell factors was performed to obtain red blood cell counts, hemoglobin, hematocrit, and the size of the red blood cells (mean corpuscular volume) using an automated blood cell counter (Hemavet 950FS, DrewScientific, Waterbury, CT, USA)

Determination of heme levels:

The assay was carried out as it was reported in the literature with minor modifications (To-Figueras et al., 2003). This method is based upon the conversion of the protein's heme moiety to its fluorescent porphyrin derivative by incubation with oxalic acid. For this assay, we used mouse liver homogenates of $CSE^{-/-}$ and wild-type mice prepared in 1xMSHE solution supplemented with protease inhibitors. For plasma collection, we used EDTA solution. We added 400 µl 2M oxalic acid solution in reaction with 30µl EDTA-plasma or 30µl / 30µg liver homogenate samples while incubating the samples in the dark. The samples then were heated to 100 °C for 30 min and then cooled to RT for 15 min, and lastly centrifuged at 20,000g at 4°C for 10 min to remove the debris. Protoporphyrin IX (PpIX) was measured in the supernatant at 405nm excitation and 600nm emission wavelengths. Samples treated with oxalic acid but not subjected to heat were served as controls to determine the basal endogenous/free PpIX level in each sample. A calibration curve was prepared using a range of concentrations of PpIX. The fluorescence of the solutions was stable for over 24 hours at room temperature in daylight.

Determination of arterial and venous blood gases:

Arterial and venous blood gases were determined by using RAPID point® 500 System (Siemens Healthcare Diagnostics, Inc, Tarrytown, NY, USA). Briefly, animals were anesthetized by isoflurane using medical air supply. Arterial blood was drawn from the left atrium of the heart. Then, venous blood was taken from the inferior vena cava. The blood was collected in previously heparinized tubes.

Short-term survival study:

Male $CSE^{-/-}$ and wild-type mice were placed into a custom hypoxic cabinet and subjected to 5% hypoxia for a short-term survival study (Coy Laboratory Products, Grass Lake, MI, USA). The hypoxic cabinet was supplied with O_2 and N_2 using controllers. The chamber was set up to 5% O_2 and 95% N_2 atmosphere.

Real-time PCR:

Total RNA was isolated from liver tissue using TRIzol (Sigma-Aldrich, St. Louis, MO, USA), and treated with RNase-free DNase (New England BioLabs, Ipswich, MA, USA). Reverse transcription was performed using the Maxima First Strand cDNA Synthesis system (Thermo Fisher Scientific, Waltham, MA, USA). The relative abundance of mRNA in each sample was measured by real-time PCR in a fluorescent temperature cycler (CFX96 Real-

Time PCR Detection System) with SYBR Green PCR Master Mix (Bio-Rad). Mouse primers for coproporphyrinogen oxidase (CPOX), ferrochelatase, uroporphyrinogen decarboxylase (UROD), ALA dehydratase, and GAPDH were used, and the sequences are listed below. The specificity of PCR was determined by melt-curve analysis for each reaction. The relative difference in mRNA between samples was calculated using the arithmetic formula $2^{-\Delta\Delta CT}$.

Western blotting:

Cells were lysed in Nonidet P-40 buffer (50 mmol/L Tris-HCl pH 8.0, 150 mmol/L NaCl, 1% Nonidet P-40) and mouse tissue samples were homogenized in radioimmunoprecipitation assay (RIPA) buffer both supplemented with protease and phosphate inhibitors, diluted in NuPAGE LDS Sample Buffer (Thermo Fisher Scientific, Waltham, MA, USA), and boiled. Lysates (25 g protein/10 μl/well) were resolved on 4–12% NuPage Bis-Tris acrylamide gels (Thermo Fisher Scientific, Waltham, MA, USA) and transferred to PVDF membranes. Membranes were blocked with Starting Block T20 (Thermo Fisher Scientific, Waltham, MA, USA) and then were probed overnight with primary antibodies; anti-CSE/CBS/GAPDH/TST (1:1000; Proteintech Group Inc., Chicago, IL, USA), anti-3-MST antibody (1:1000; Sigma-Aldrich, St. Louis, USA), anti-Tom20 and anti-CPOX (Santa Cruz Biotechnology, Dallas, TX, USA). On the following day, anti-rabbit/mouse horseradish peroxidase-conjugated secondary antibody (1:3,000; Cell Signaling, Danvers, USA) was applied. The enhanced chemiluminescent substrate (Pierce Biotechnology, Thermo Fisher Scientific, Waltham, MA, USA) was used to detect the signal in a camera-based chemiluminescence detection system (Alpha Innotech MultiImage II Alphaimager HP, ProteinSimple, San Jose, CA, USA). To normalize signals, the membranes were re-probed with β-actin and GAPDH antibodies (1:3,000; Sigma-Aldrich or Proteintech Group Inc). The intensity of Western blot signals was quantified by densitometry using the ImageJ 1.45s software (U.S. National Institutes of Health, Bethesda, MD, USA). The ratios of the signals were expressed as normalized densitometry units.

In a separate experiment, we used Total OXPHOS Rodent WB Antibody Cocktail (ab110413, Abcam, Cambridge, United Kingdom) against CI subunit NDUFB8 (ab110242), CII-30kDa (ab14714), CIII-Core protein 2 (ab14745) CIV subunit I (ab14705) and CV alpha subunit (ab14748) as an optimized premixed cocktail. This assay was suitable for Western blotting analysis of the relative levels of these five OXPHOS complexes in liver homogenates of $CSE^{-/-}$ and wild-type mice.

Detection of CSE-derived H_2S production in liver tissue:

The assay was carried out on a 96-well plate format, in a total assay volume of 200 μl as described (Druzhyna et al., 2016). The tissues samples were homogenized in ice-cold NP40 lysing buffer (1%NP40; 150 mM NaCl; 50mM Tris-Cl, pH 8.0) supplemented with protease inhibitor for 30 min on ice before centrifugation. For measurement of CSE activity, we added L-cysteine (10 mM), the substrate of CSE. Separately, the L-cysteine–induced increased in CSE activity was blocked by the addition of PAG (3 mM), the CSE inhibitor. The difference in the H_2S production between these two groups determined the enzymatic CSE-derived H_2S production. Pyridoxal 5'-phosphate (PLP, 5 μM) was also added to the

reaction as a cofactor of the enzyme. Finally, an H_2S-specific fluorescent probe 7-azido-4-methylcoumarin (AzMc, 10 μM) was used to scavenge H_2S. The mixture was incubated at 37 °C for 2 hours, and the fluorescence of the mixture was read at 450 nm (λex = 365 nm).

Determination of porphyrins by HPLC:

A Perkin Elmer Series 200 HPLC system (Waltham, MA, USA) with a Bondclone 10 μm C18 148 A, 150 mm x 3.9 mm LC column with UV/Visible and fluorescence detectors was used for analysis (Phenomenex Inc., Torrance, CA, USA). The components of Mobile Phase A (pH= 5.16) contained 27.5 ml glacial acetic acid, 22.5 ml concentrated ammonium hydroxide and 50 ml acetonitrile in 500 ml total volume of Milli-Q water. The components of Mobile Phase B contained 50 ml acetonitrile and 450 ml methanol in 500 ml total volume.

For the identification of porphyrin carboxylic acids, a chromatographic marker kit containing an equimolar mixture of porphyrin 8-, 7-, 6-, 5-, 4-, and 2-carboxylic acids was applied (Frontier Scientific, Inc., Salt Lake City, UT, USA). This was labeled as HIGH standards mix (one nmol/mL of each porphyrin carboxylic acid). Urine specimens were vortexed well. One ml aliquots of the supernatants were pipetted out and mixed with 50 microliters of concentrated hydrochloric acid, vortexed well, centrifuged, and the supernatants were transferred to auto-sampler vials. A gradient elution program was used with the injection volume set to 100 μl and total run time to 36 minutes (To-Figueras et al., 2003; Lim and Peters, 1984). High and low concentration standard solution of porphyrin carboxylic acids were analyzed with each batch of samples to identify amounts of individual porphyrins.

Porphyrin standard mixtures that contained equal amounts of uroporphyrin, heptacarboxyl porphyrin, hexacarboxyl porphyrin, pentacarboxyl porphyrin, coproporphyrin and mesoporphyrin (an alternative dicarboxyl porphyrin to protoporphyrin, which is less stable). The high standard mixture was diluted 14-fold to prepare the lower standard mixture. Acceptable limits of variability were ± 10% of the predetermined mean value for porphyrin carboxylic acid peaks in the standards.

Bioenergetic analysis in isolated liver mitochondria:

The XF24 Extracellular Flux Analyzer (Agilent, Santa Clara, USA) was used to measure bioenergetic function in isolated mouse liver mitochondria and intact HepG2 cells as described (Modis et al., 2013). Mitochondrial assay solution 1 (MAS-1) comprised 70 mM sucrose, 220 mM mannitol, 10 mM KH_2PO_4, 5 mM $MgCl_2$, 2 mM HEPES, 1 mM EGTA, and 0.2% (w/v) fatty acid-free BSA (pH 7.2) at 37°C. Respiration by mitochondria (10 μg/well) was sequentially measured in a coupled state with substrate present (basal respiration, State 2), followed by State 3 (phosphorylating respiration, in the presence of ADP and substrate), State 4 (non-phosphorylating or resting respiration) following conversion of ADP to adenosine triphosphate (ATP), State 4o, induced with the addition of oligomycin. Next, maximal uncoupler-stimulated respiration (State 3u) was detected by the administration of the uncoupling agent FCCP. At the end of the experiment the Complex III inhibitor, antimycin A was applied to completely shut down the mitochondrial respiration.

In the second set of studies, electron flow experiments were conducted. This method allows the functional assessment of selected mitochondrial complexes together in the same time frame. Mitochondrial electron transport was stimulated by the addition of pyruvate/malate (10 mM/2 mM, respectively, in order to enable the activity of all complexes); with succinate (10 mM, in the presence of the Complex I inhibitor rotenone, 2 μM, in order to direct the electron flow exclusively through complexes II, III and IV) or with the artificial substrates ascorbate/TMPD (10 mM/100 μM, respectively, in the presence of the Complex III inhibitor antimycin at 4 μM, in order to selectively activate Complex IV).

Bioenergetic analysis in intact liver cells:

Prior to the bioenergetic measurements – conducted as described (Modis et al., 2013), the culture medium was changed to unbuffered DMEM lacking serum. After transiently silencing the CSE and CPOX genes, we measured the changes in oxygen consumption rate (OCR) for subsequent experiments. Next, a protocol was implemented to measure indices of mitochondrial function. Oligomycin, FCCP (carbonyl cyanide 4-(trifluoromethoxy) phenylhydrazone), and antimycin A/rotenone (AA + Rot) were injected sequentially through ports of the Seahorse Flux Pak cartridges to reach 1.5 μM, 0.5 μM, 2 μg/ml and 2 μM, respectively. Key bioenergetic parameters such as basal respiration (resting cell respiration), ATP production (calculated from the drop in OCR, in response to the ATP-synthase inhibitor, oligomycin), proton leak (migrated protons to the matrix without producing ATP, basal/inducible proton leak), maximal respiratory capacity (maximal oxygen consumption achievable by using the uncoupling agent FCCP), and spare respiratory capacity (accessible mitochondrial reserve capacity under high bioenergetic demands) were measured.

CPOX reporter system:

The LightSwitch Luciferase Assay System for obtaining CPOX reporter assay results was used according to manufacturer's instructions (SWITCHGEAR GENOMICS, Carlsbad, CA, USA).

Statistical analysis:

Data are shown as mean ± SEM. Statistical analyses included Student's t-test, one-way, or two-way ANOVA followed by Dunnett's multiple comparisons to detect differences between groups. Statistical analysis was performed using GraphPad Prism 7 analysis software (GraphPad Software Inc., La Jolla, CA, USA). The experiments were repeated independently at least 3 times, performed on three different experimental days, with at least 3 replicates of each assay group or condition on a single experimental day. A value of $*p<0.05$ or $**p<0.01$ was considered statistically significant.

3. Results

$CSE^{-/-}$ mice exhibit elevated red blood cell counts

Analysis of blood samples from $CSE^{-/-}$ mice revealed significantly elevated red blood cell (RBC) counts, hemoglobin, and hematocrit parameters compared to the wild-type control group (Figure 1). The mean corpuscular volume (MCV) of RBCs — a parameter for

determining the size of the RBCs — was also elevated, suggesting increased hemoglobin content in RBCs.

$CSE^{-/-}$ mice exhibit elevated plasma and liver heme levels

To measure the heme moiety of plasma and liver proteins, we used a fluorometric procedure during which the heme is converted into its fluorescent porphyrin derivative, protoporphyrin IX (Figure 2). We found that the heme/protoporphyrin IX levels of both plasma and liver homogenates were elevated by 1.2- and 1.3-fold in $CSE^{-/-}$ mice.

$CSE^{-/-}$ mice do not demonstrate significant alterations in arterial or venous blood gas parameters

To determine if the elevated RBC content in $CSE^{-/-}$ mice produces altered blood gas parameters, we collected blood from anesthetized mice receiving medical air (21% FiO_2). Glucose, HCO_3, pO_2, pCO_2, lactate, pH, and total hemoglobin were measured under resting conditions (Table 3). No significant differences in these parameters were noted between the experimental groups, except for hemoglobin level, which was significantly increased in the $CSE^{-/-}$ group. Both the shunt fraction, calculated from the changes between venous and arterial blood, and the PaO_2/FiO_2 ratio were also similar in $CSE^{-/-}$ and wild-type groups.

Absence of CSE does not affect tolerance to severe global hypoxia *in vivo*

Next, we determined whether the elevated RBC content in $CSE^{-/-}$ mice produces a difference in hypoxia tolerance. $CSE^{-/-}$ and wild-type mice were subjected to 5% hypoxia for a short-term survival study. Mice were monitored and data were recorded every minute. There were no significant differences between the survival of $CSE^{-/-}$ mice (n=27) *vs.* their wild-type controls (n=30) (Figure 3).

$CSE^{-/-}$ mice exhibit elevated CPOX expression in the liver

We hypothesized that the altered RBC parameters in $CSE^{-/-}$ mice could be explained by potential changes in the heme biosynthesis pathway. Therefore, we tested gene expression levels of four principal enzymes involved in the heme biosynthesis pathway. We found that the mRNA level of CPOX, the sixth enzyme involved in heme biosynthesis, was significantly elevated in the liver tissue of $CSE^{-/-}$ mice (Figure 4). The mRNA expression level of ferrochelatase, the terminal enzyme of the heme biosynthetic pathway tended to also increase, but the difference did not reach statistical significance ($p = 0.054$). Expression levels of uroporphyrinogen decarboxylase and ALA dehydratase were not altered. In accordance with the mRNA expression data, significantly elevated CPOX protein expression was noted in the liver of $CSE^{-/-}$ mice using Western blotting (Figure 5A, B).

Absence of CSE does not affect the expression of other enzymes involved in H_2S production

Neither the expression level of the other two H_2S-producing enzymes CBS and 3-MST, nor the expression of the principal H_2S-degrading enzyme TST was affected by CSE deficiency. Tom 20, a 20 kDa mitochondrial outer membrane protein was significantly elevated in liver homogenates from $CSE^{-/-}$ mice, perhaps indicative of increased mitochondrial biogenesis.

As expected, CSE expression, as well as CSE-dependent H_2S production were completely absent in liver tissue homogenates of $CSE^{-/-}$ mice (Figure 5).

Perturbed porphyrin metabolism in $CSE^{-/-}$ mice

To investigate the distribution of porphyrin derivates and to accurately determine the enzyme activity of CPOX, we measured various porphyrin intermediaries in urine samples of $CSE^{-/-}$ and wild-type mice by HPLC (Table 1). Among all the porphyrin derivates, the level of coproporphyrinogen (measured as coproporphyrin, its oxidized form) was prominently detectable in both groups. Uroporphyrinogen (measured as uroporphyrin) was also detected; however other porphyrins were, as expected, found only in trace amounts.

We confirmed reduced levels of coproporphyrins I and III (oxidized forms of coproporphyrinogen I and III) in urine samples from $CSE^{-/-}$ mice compared to wild-type mice, suggesting increased CPOX enzyme activity and utilization of the substrate coproporphyrinogen III in $CSE^{-/-}$ tissues (Figure 6A). Additionally, uroporphyrinogen - the substrates of UROD enzyme, uroporphyrinogen I and III are two distinct metabolic isomers of uroporphyrinogen - was significantly elevated in urine samples of $CSE^{-/-}$ mice (Figure 6B). The level of coproporphyrinogen depends on both UROD and CPOX enzyme activities. Therefore, a possible explanation of our findings is that CPOX activity increases relative to UROD activity following increased CPOX mRNA/protein expression, which may accelerate heme production in $CSE^{-/-}$ mice.

Enhanced mitochondrial function in liver mitochondria isolated from $CSE^{-/-}$ mice

Several mitochondrial electron transport chain (ETC) proteins are heme-dependent and therefore depend on porphyrin-heme biosynthesis. To determine whether the elevated heme content in liver tissues of $CSE^{-/-}$ mice alters the mitochondrial function, we isolated mitochondria from liver homogenates using differential centrifugation (Figure 7A). Tom 20, a marker for mitochondrial biogenesis, was elevated in liver homogenates from $CSE^{-/-}$ mice. Expression of CPOX was significantly higher in mitochondria from $CSE^{-/-}$ mice. GAPDH protein was present in the mitochondria-enriched fractions, perhaps due to a small degree of cytosolic contamination of the preparation – and/or due to mitochondrial GAPDH, which has been described in several reports (e.g. Kohnr et al., 2014). The presence of CBS in both the homogenates and mitochondria-enriched fractions was consistent with the results from Teng and colleagues showing that CBS proteins are present in liver mitochondria at a low level under baseline conditions (Teng et al., 2013).

In terms of bioenergetic readouts, the absence of CSE resulted in significant enhancement of the mitochondrial function based on different bioenergetic measurements (‘coupling’ and ‘electron flow’ assays) in isolated mouse liver mitochondria *ex vivo* (Figure 7B, C). This ‘coupling assay’ examines the degree of coupling between the ETC and the oxidative phosphorylation (OXPHOS), to determine mitochondrial function/dysfunction. We found that state 3, 4o, and 3u respiration were significantly elevated in isolated liver mitochondria from $CSE^{-/-}$ mice. Modified electron flow experiments demonstrated that the absence of CSE in isolated liver mitochondria-enriched fraction exerted a stimulatory effect, when Complexes I–IV or II–IV or Complex IV alone were functioning simultaneously (Figure 7D,

E). There is a well-known inhibitory effect of H_2S on Complex IV activity (reviewed in Szabo et al., 2014). It is conceivable that this may exert a tonic inhibitory effect on mitochondrial electron transport; thus, the absence of CSE-derived H_2S generation may result in increased Complex IV activity.

Absence of CSE does not affect the expression level of mitochondrial complexes

To investigate whether the higher heme content in liver tissues of $CSE^{-/-}$ mice results in altered expression level of mitochondrial complexes, we performed Western blot analysis to assess the protein levels of all mitochondrial complexes. We found no differences in the expression levels of any of these complexes in liver tissue homogenates between $CSE^{-/-}$ and wild-type mice (Figure 8).

Attenuation of CSE expression stimulates mitochondrial respiration in cultured hepatocytes in a partially CPOX-dependent fashion

SiRNA-mediated transient silencing of CSE resulted in an enhanced mitochondrial respiration in HepG2 cultures (Figure 9). Attenuation of CPOX expression by siRNA significantly decreased respiratory responses in liver cells. In cells with CPOX silencing, the CSE-silencing-induced stimulation of mitochondrial respiration was attenuated when compared cells with intact CSE (Figure 9).

CSE and H_2S regulate CPOX gene promoter activity in cultured hepatocytes

To understand the mechanisms by which the CPOX gene is regulated by the CSE/H_2S pathway, we measured CPOX promoter activity. We transfected the HepG2 liver cells by CPOX luciferase reporter construct and treated the cells with an H_2S-donor compound (NaHS) or an irreversible pharmacological inhibitor of CSE (propargylglycine; PAG) (Szabo and Papapetropoulos, 2017). Addition of NaHS suppressed CPOX promoter activity, whereas PAG exerted a stimulatory effect (Figure 10). These results indicate that H_2S regulates COPX gene/promoter activity. Exogenous H_2S inhibits COPX gene expression while blocking CSE and subsequently suppressing endogenous H_2S production result in increased COPX promoter activity. Decreased endogenous H_2S availability could eventually lead to elevated COPX protein expression.

4. Discussion

The main findings of the current report can be summarized as follows: (1) $CSE^{-/-}$ mice exhibit elevated red blood cell counts and red blood cell MCVs compared to wild-type mice; (2) these changes are associated with increased plasma and liver heme levels and (3) these alterations are likely due to an induction of CPOX which (4) – based on *in vitro* promoter data - may be directly influenced by H_2S, the product of CSE. With respect to the potential functional relevance of these findings, (5) the increased circulating red blood cell numbers do not correspond to any detectable alterations in blood gas parameters under resting conditions, (6) nor do they affect the hypoxia tolerance of the animals in an acute severe hypoxia model. However, there may be a functional interaction between the CSE system and CPOX in terms of mitochondrial bioenergetics: (7) $CSE^{-/-}$ hepatocytes and mitochondria isolated from them exhibit increased oxidative phosphorylation parameters, and (8) this

increase is partially blunted after CPOX silencing. However, although heme is essential for the biosynthesis of mitochondrial electron chain complexes, and CPOX is required for heme biosynthesis, (9) the observed functional mitochondrial alterations were not associated with detectable changes in expression levels of mitochondrial ETC proteins.

With respect to the *in vivo* blood gas and hypoxia tolerance data, the most likely interpretation of the current findings is that the relatively minor alterations in red blood cell parameters seen in the $CSE^{-/-}$ mice are not sufficient to produce any functional change in terms of oxygen delivery to the tissues or global blood gas parameters, in resting conditions, or in a model of acute severe hypoxia. Under hypoxia conditions, the limiting factor for oxygen delivery or animal survival is the availability of oxygen supply, not the oxygen affinity of hemoglobin nor the RBC content. As such, although $CSE^{-/-}$ mice have increased RBC content, these mice cannot be benefited from the increased oxygen binding capacity of their RBCs, nor resuscitated from hypoxia. However, these findings do not exclude the possibility that in other models – e.g. during chronic hypoxia, or in disease models that have chronic hypoxia or hypoxemia as a component – the same differences in blood gas parameters may produce detectable changes. This possibility remains to be investigated in future experiments.

In the literature, there were several reports linking H_2S, or various H_2S-biosynthetic pathways to hypoxic responses or hypoxic tolerance. For instance, mice placed in H_2S environment were reported to develop a suspended animation-like state (Blackstone et al, 2005), although subsequent studies have questioned the methodology and the interpretation, as well as the scalability and potential translatability of these observations (Li et al., 2008; Hartmann et al., 2017, Hemelrijk et al., 2018). There are several reports linking hypoxia-responsiveness of various cell types to the H_2S (and its various endogenous sources, including CSE) (Li et al., 2014; Guo et al., 2015; Tao et al., 2017); at least in some experimental system, hypoxia was noted to increase CSE expression (Wang et al., 2014). There is also a separate line of studies linking hypoxia-sensing to the CSE/H_2S system in the carotid body (Peng et al., 2010; Prabhakar, 2012; Peng et al., 2019). There are also reports suggesting that H_2S can induce erythropoietin synthesis (Leigh et al., 2016; Leigh et al., 2018). However, the potential relationship of the current findings with the above-listed body of literature is presently unclear. It should be also mentioned that increased red blood cell count does not always or does not necessarily confer protective effects; for example, higher red blood cell count could theoretically induce an enhanced incidence of thrombosis and stroke when subjected to hypoxia (experiments in this direction remain to be conducted in the future). With these unknowns, we must conclude that the question whether CSE deficiency provides an advantage to hypoxia tolerance remains undetermined.

There are many additional issues and potential experimental directions that we did not address in the current study, but which may be interesting and should be explored in the future. For example, it would be interesting to explore whether the H_2S system may have any influence on the levels of 2,3-biphosphate-glycerate (2,3-DPG) in the erythrocytes, because this factor can control affinity of heme groups by oxygen. Currently there are no publications regarding to potential interrelationships between H_2S and 2,3-DPG.

According to our present findings, the induction of heme and erythropoiesis was associated with an upregulation of CPOX (mRNA and protein) in $CSE^{-/-}$ mice (while none of the other examined enzymes in the heme biosynthesis showed any significant change). CPOX, a mitochondrial enzyme (Sano and Granick, 1961; Kohno et al., 1993) is one of the eight enzymes essential for heme biosynthesis. Its deficiency in hereditary coproporphyria (HCP) is due to inherited CPOX mutations, causing neurologic and cutaneous symptoms that result from accumulation of pathway intermediates (Martasek et al., 1994; Lamoril et al., 1995; Heyer et al., 2006). Whether in-born or acquired alterations in CSE expression or activity in the liver may influence severity of this hepatic porphyria by modulating the expression of hepatic CPOX mRNA as well as protein warrants investigation. Because heme is essential for a function of a variety of hemoprotein enzymes and other hemoproteins, changes in heme biosynthesis in HCP might influence a host of biological functions. While we did not observe detectable effects on the level of blood gas parameters, there were changes in the mitochondrial functional measurements: CPOX silencing suppressed mitochondrial electron transport and oxygen consumption (both basally and after uncoupling the mitochondria with FCCP). Moreover, CPOX silencing attenuated the CSE-deficiency-induced increase in mitochondrial electron transport. One possible interpretation of the latter finding is that CSE-deficiency, at least in part, may induce the increase in mitochondrial function by upregulating CPOX, and thereby increasing mitochondrial heme content (including the heme content of electron transport proteins), and this upregulation effect (and therefore the stimulatory effect on mitochondrial electron transport) is suppressed when CPOX is silenced. However, other interpretations of these findings are also conceivable. It will be interesting to examine, in follow-up studies, whether the observed alterations in mitochondrial function in $CSE^{-/-}$ mice also translate to altered metabolic function (e.g. potential increases in whole-body oxygen consumption).

Regardless of its connection to CPOX pathway, the very fact that $CSE^{-/-}$ liver mitochondria and hepatocytes after $CSE^{-/-}$ silencing exhibit increased mitochondrial function is also very interesting. In the field of environmental toxicology, H_2S has been long considered an inhibitor of mitochondrial function, due to its inhibitory effect on mitochondrial Complex IV (cytochrome c oxidase), where it acts as a potent, reversible inhibitor (reviewed in Nicholls et al., 2013; Szabo et al., 2014). However, according to most studies, these inhibitory effects are only relevant at high (supraphysiological, toxicological) concentrations. There are also several lines of data demonstrating that at lower (i.e. endogenous, physiologically relevant) concentrations of H_2S, there is a stimulatory effect of this transmitter on mitochondrial function, due to a combination of mechanisms (direct electron donation at Complex IV, inhibition of intramitochondrial phosphodiesterases, stimulation of ATP synthase via sulfhydration) (Szabo et al., 2014; Modis et al., 2016). However, the current findings – at least in the tissue/cell type studied here, i.e. the liver/hepatocyte - suggest that the endogenous H_2S effect is, in fact a basal inhibitory effect of mitochondrial function. It should be pointed out that there are diverse reports in the literature with respect to the role of CSE in the regulation of mitochondrial function. For instance, in murine adrenocortical cells either CBS/CSE inhibitors or small interfering RNAs lead to mitochondrial oxidative stress and dysfunction (Wang et al., 2014) and in hepatoma HepG2 and PLC/PRF/5 cells inhibition of the endogenous H_2S/CSE pathway was found to enhance ROS production, induce

mitochondrial disruption and decrease cell proliferation (Pan et al., 2014). In other cell types (e.g. in smooth muscle cells), $CSE^{-/-}$ phenotype confers suppressed mitochondrial function under basal and especially under stimulated conditions (e.g. in response to cellular calcium mobilization) (Pan et al., 2012). Taken together, the functional role of the $CSE^{-/-}$ phenotype likely depends on the cell type as well as the context (experimental condition, type of stimulus, short- vs. long-term observation, etc.)

In conclusion, the current findings indicate that the CSE system regulates the expression of CPOX and consequent heme synthesis (Fig. 11). These effects in turn, do not influence global oxygen transport parameters, but may regulate mitochondrial electron transport.

Acknowledgments

Funding

This work was supported by the Postdoctoral Fellowship of the Canadian Institutes of Health Research (201302MFE-299117-233866) and the Scientist Development Grant of the American Heart Association (16SDG29860009) to KM. The project was also benefited from additional funding sources; Natural Sciences and Engineering Research Council of Canada (RGPIN-2017-04392) to R.W., National Institutes of Health (R01CA175803) to C.S. and the Swiss National Foundation (31003A_179434) to C.S.

Availability of data and materials

The datasets used and/or analyzed during the current study are available from the corresponding author on reasonable request.

Abbreviations

ADP	Adenosine 5’-diphosphate
ATP	Adenosine 5’-triphosphate
AUC	Area-under-the-curve
AzMc	7-Azido-4-methylcoumarin
2,3-DPG	2,3-Biphosphate-glycerate
FCCP	Carbonyl cyanide 4-(trifluoromethoxy) phenylhydrazone
CPOX	Coproporphyrinogen oxidase gene and protein
CBS	Cystathionine beta-synthase
CSE	Cystathionine gamma-lyase
DMEM	Dulbecco’s modified Eagle’s medium
ETC	Electron transport chain
EPO	Erythropoietin
GAPDH	Glyceraldehyde 3-phosphate dehydrogenase

HPLC	High Performance Liquid Chromatography
H_2S	Hydrogen sulfide
MCV	Mean corpuscular volume
3-MST	3-Mercaptopyruvate sulfurtransferase
TMPD	N,N,N′,N′-tetramethyl-p-phenylenediamine dihydrochloride
PLP	Pyridoxal 5’-phosphate
RBC	Red blood cell
TST	Rhodanese
OXPHOS	Oxidative phosphorylation
UROD	Uroporphyrinogen decarboxylase gene and protein

References

(1). Ahmad A, Druzhyna N, Szabo C, Cystathionine-gamma-lyase deficient mice are protected against the development of multiorgan failure and exhibit reduced inflammatory response during burn, Burns 43 (5) (2017) 1021–1033. [PubMed: 28318752]

(2). Ahmad A, Gerö D, Olah G, Szabo C, Effect of endotoxemia in mice genetically deficient in cystathionine-γ-lyase, cystathionine-β-synthase or 3-mercaptopyruvate sulfurtransferase, Int. J. Mol. Med 38 (6) (2016) 1683–1692. [PubMed: 27748832]

(3). Ang AD, Rivers-Auty J, Hegde A, Ishii I, Bhatia M, The effect of CSE gene deletion in caerulein-induced acute pancreatitis in the mouse, Am. J. Physiol. Gastrointest. Liver Physiol 305 (10) (2013) G712–21. [PubMed: 24008358]

(4). Bibli SI, Hu J, Sigala F, Wittig I, Heidler J, Zukunft S, Tsilimigras DI, Randriamboavonjy V, Wittig J, Kojonazarov B, Schürmann C, Siragusa M, Siuda D, Luck B, Abdel Malik R, Filis KA, Zografos G, Chen C, Wang DW, Pfeilschifter J, Brandes RP, Szabo C, Papapetropoulos A, Fleming I, Cystathionine γ lyase sulfhydrates the RNA binding protein human antigen R to preserve endothelial cell function and delay atherogenesis, Circulation 139 (1) (2019) 101–114. [PubMed: 29970364]

(5). Blackstone E, Morrison M, Roth MB, H_2S induces a suspended animation-like state in mice, Science 308 (5721) (2005) 518. [PubMed: 15845845]

(6). Coletta C, Modis K, Olah G, Brunyanszki A, Herzig DS, Sherwood ER, Ungvari Z, Szabo C, Endothelial dysfunction is a potential contributor to multiple organ failure and mortality in aged mice subjected to septic shock: preclinical studies in a murine model of cecal ligation and puncture, Crit. Care 18 (5) (2014) 511. [PubMed: 25223540]

(7). Coletta C, Papapetropoulos A, Erdelyi K, Olah G, Módis K, Panopoulos P, Asimakopoulou A, Gerö D, Sharina I, Martin E, Szabo C, Hydrogen sulfide and nitric oxide are mutually dependent in the regulation of angiogenesis and endothelium-dependent vasorelaxation, Proc. Natl. Acad. Sci. USA 109 (23) (2012) 9161–9166. [PubMed: 22570497]

(8). Druzhyna N, Szczesny B, Olah G, Modis K, Asimakopoulou A, Pavlidou A, Szoleczky P, Gero D, Yanagi K, Toro G, Lopez-Garcia I, Myrianthopoulos V, Mikros E, Zatarain JR, Chao C, Papapetropoulos A, Hellmich MR, Szabo C, Screening of a composite library of clinically used drugs and well-characterized pharmacological compounds for cystathionine beta-synthase inhibition identifies benserazide as a drug potentially suitable for repurposing for the experimental therapy of colon cancer, Pharmacol. Res 113 (Pt A) (2016) 18–37. [PubMed: 27521834]

(9). Fu M, Zhang W, Wu L, Yang G, Li H, Wang R, Hydrogen sulfide (H2S) metabolism in mitochondria and its regulatory role in energy production, Proc. Natl. Acad. Sci. USA 109 (8) (2012) 2943–2948. [PubMed: 22323590]

(10). Gaddam RR, Fraser R, Badiei A, Chambers S, Cogger VC, Le Couteur DG, Ishii I, Bhatia M, Cystathionine-gamma-lyase gene deletion protects mice against inflammation and liver sieve injury following polymicrobial sepsis, PLoS One 11 (8) (2016) e0160521. [PubMed: 27518439]

(11). Guo W, Li D, You Y, Li W, Hu B, Zhang S, Miao L, Xian M, Zhu Y, Shen X, Cystathionine γ-lyase deficiency aggravates obesity-related insulin resistance via FoxO1-dependent hepatic gluconeogenesis, FASEB J. 33 (3) (2019) 4212–4224. [PubMed: 30526049]

(12). Guo Z, Li CS, Wang CM, Xie YJ, Wang AL, CSE/H2S system protects mesenchymal stem cells from hypoxia and serum deprivation-induced apoptosis via mitochondrial injury, endoplasmic reticulum stress and PI3K/Akt activation pathways, Mol. Med. Rep 12 (2) (2015) 2128–2134. [PubMed: 25901909]

(13). Hartmann C, Nussbaum B, Calzia E, Radermacher P, Wepler M, Gaseous mediators and mitochondrial function: the future of pharmacologically induced suspended animation? Front. Physiol 8 (2017) 691. [PubMed: 28974933]

(14). Hemelrijk SD, Dirkes MC, van Velzen MHN, Bezemer R, van Gulik TM, Heger M, Exogenous hydrogen sulfide gas does not induce hypothermia in normoxic mice, Sci. Rep 8 (1) (2018) 3855. [PubMed: 29497053]

(15). Hesketh EE, Czopek A, Clay M, Borthwick G, Ferenbach D, Kluth D, Hughes J, Renal ischaemia reperfusion injury: a mouse model of injury and regeneration, J. Vis. Exp (88) (2014).

(16). Heyer NJ, Bittner AC, Echeverria D, Woods JS, A cascade analysis of the interaction of mercury and coproporphyrinogen oxidase (CPOX) polymorphism on the heme biosynthetic pathway and porphyrin production, Toxicol. Lett 161 (2) (2006) 159–166. [PubMed: 16214298]

(17). Huang CW, Moore PK, H_2S synthesizing enzymes: biochemistry and molecular aspects, Handb. Exp. Pharmacol 230 (2015) 3–25. [PubMed: 26162827]

(18). Ishii I, Akahoshi N, Yamada H, Nakano S, Izumi T, Suematsu M, Cystathionine gamma-lyase-deficient mice require dietary cysteine to protect against acute lethal myopathy and oxidative injury, J. Biol. Chem 285 (34) (2010) 26358–26368. [PubMed: 20566639]

(19). Kimura H, Signaling molecules: hydrogen sulfide and polysulfide, Antioxid. Redox. Signal 22 (5) (2015) 362–376. [PubMed: 24800864]

(20). Kohno H, Furukawa T, Yoshinaga T, Tokunaga R, Taketani S, Coproporphyrinogen oxidase. Purification, molecular cloning, and induction of mRNA during erythroid differentiation, J. Biol. Chem 268 (28) (1993) 21359–21363. [PubMed: 8407975]

(21). Kohr MJ, Murphy E, Steenbergen C, Glyceraldehyde-3-phosphate dehydrogenase acts as a mitochondrial trans-S-nitrosylase in the heart, PLoS One 9 (10) (2014) e111448. [PubMed: 25347796]

(22). Lamoril J, Martasek P, Deybach JC, Da Silva V, Grandchamp B, Nordmann Y, A molecular defect in coproporphyrinogen oxidase gene causing harderoporphyria, a variant form of hereditary coproporphyria, Human Mol. Gen 4 (2) (1995) 275–278.

(23). Leigh J, Juriasingani S, Akbari M, Shao P, Saha MN, Lobb I, Bachtler M, Fernandez B, Qian Z, Van Goor H, Pasch A, Feelisch M, Wang R, Sener A, Endogenous H2S production deficiencies lead to impaired renal erythropoietin production, Can. Urol. Assoc. J (2019) In press.

(24). Leigh J, Saha MN, Mok A, Champsi O, Wang R, Lobb I, Sener A, Hydrogen sulfide induced erythropoietin synthesis is regulated by HIF proteins, J. Urol 196 (1) (2016) 251–260. [PubMed: 26880412]

(25). Li C, Guo Z, Guo B, Xie Y, Yang J, Wang A, Inhibition of the endogenous CSE/H_2S system contributes to hypoxia and serum deprivation-induced apoptosis in mesenchymal stem cells, Mol. Med. Rep 9 (6) (2014) 2467–2472. [PubMed: 24699897]

(26). Li H, Mani S, Wu L, Fu M, Shuang T, Xu C, Wang R, The interaction of estrogen and CSE/H_2S pathway in the development of atherosclerosis, Am. J. Physiol. Heart Circ. Physiol 312 (3) (2017) H406–H414. [PubMed: 27986657]

(27). Li J, Zhang G, Cai S, Redington AN, Effect of inhaled hydrogen sulfide on metabolic responses in anesthetized, paralyzed, and mechanically ventilated piglets, Pediatr. Crit. Care Med. 9 (1) (2008) 110–112. [PubMed: 18477923]

(28). Lim CK, Peters TJ, Urine and faecal porphyrin profiles by reversed-phase high-performance liquid chromatography in the porphyrias, Clin. Chim. Acta 139 (1984) 55–63. [PubMed: 6723073]

(29). Liu S, Wang X, Pan L, Wu W, Yang D, Qin M, Jia W, Xiao C, Long F, Ge J, Liu X, Zhu Y, Endogenous hydrogen sulfide regulates histone demethylase JMJD3-mediated inflammatory response in LPS-stimulated macrophages and in a mouse model of LPS-induced septic shock, Biochem. Pharmacol 149 (2018) 153–162. [PubMed: 29074105]

(30). Mani S, Li H, Untereiner A, Wu L, Yang G, Austin RC, Dickhout JG, Lhoták Š, Meng QH, Wang R, Decreased endogenous production of hydrogen sulfide accelerates atherosclerosis, Circulation 127 (25) (2013) 2523–2534. [PubMed: 23704252]

(31). Martasek P, Nordmann Y, Grandchamp B, Homozygous hereditary coproporphyria caused by an arginine to tryptophane substitution in coproporphyrinogen oxidase and common intragenic polymorphisms, Human Mol. Gen 3 (3) (1994) 477–480.

(32). Módis K, Coletta C, Erdélyi K, Papapetropoulos A, Szabo C, Intramitochondrial hydrogen sulfide production by 3-mercaptopyruvate sulfurtransferase maintains mitochondrial electron flow and supports cellular bioenergetics, FASEB J. 27 (2) (2013) 601–611. [PubMed: 23104984]

(33). Módis K, Ju Y, Ahmad A, Untereiner AA, Altaany Z, Wu L, Szabo C, Wang R, S-sulfhydration of ATP synthase by hydrogen sulfide stimulates mitochondrial bioenergetics, Pharmacol. Res. 113 (Pt A) (2016) 116–124. [PubMed: 27553984]

(34). Morrison GR, Fluorometric microdetermination of heme protein, Anal. Chem. 37 (1965) 1124–1126. [PubMed: 14341592]

(35). Nicholls P, Marshall DC, Cooper CE, Wilson MT, Sulfide inhibition of and metabolism by cytochrome c oxidase, Biochem. Soc. Trans 41 (5) (2013) 1312–1316. [PubMed: 24059525]

(36). Pan Y, Ye S, Yuan D, Zhang J, Bai Y, Shao C, Hydrogen sulfide (H2S)/cystathionine γ-lyase (CSE) pathway contributes to the proliferation of hepatoma cells, Mutat. Res 763–764 (2014) 10–18.

(37). Peng YJ, Makarenko VV, Gridina A, Chupikova I, Zhang X, Kumar GK, Fox AP, Prabhakar NR, H2S mediates carotid body response to hypoxia but not anoxia, Respir. Physiol. Neurobiol 259 (2019) 75–85. [PubMed: 30086385]

(38). Peng YJ, Nanduri J, Raghuraman G, Souvannakitti D, Gadalla MM, Kumar GK, Snyder SH, Prabhakar NR, H_2S mediates O_2 sensing in the carotid body, Proc. Natl. Acad. Sci. USA 107 (23) (2010) 10719–10724. [PubMed: 20556885]

(39). Prabhakar NR, Hydrogen sulfide (H2S): a physiologic mediator of carotid body response to hypoxia, Adv. Exp. Med. Biol 758 (2012) 109–113. [PubMed: 23080150]

(40). Rogers GW, Brand MD, Petrosyan S, Ashok D, Elorza AA, Ferrick DA, Murphy AN, High throughput microplate respiratory measurements using minimal quantities of isolated mitochondria, PLoS One 6 (7) (2011) e21746. [PubMed: 21799747]

(41). Rose P, Moore PK, Zhu YZ, H_2S biosynthesis and catabolism: new insights from molecular studies, Cell. Mol. Life Sci 74 (8) (2017) 1391–1412. [PubMed: 27844098]

(42). Sano S, Granick S, Mitochondrial coproporphyrinogen oxidase and protoporphyrin formation, J. Biol. Chem 236 (1961) 1173–1180. [PubMed: 13746277]

(43). Szabo C, Ransy C, Módis K, Andriamihaja M, Murghes B, Coletta C, Olah G, Yanagi K, Bouillaud F, Regulation of mitochondrial bioenergetic function by hydrogen sulfide. Part I. Biochemical and physiological mechanisms, Br. J. Pharmacol 171 (8) (2014) 2099–2122. [PubMed: 23991830]

(44). Szijártó IA, Markó L, Filipovic MR, Miljkovic JL, Tabeling C, Tsvetkov D, Wang N, Rabelo LA, Witzenrath M, Diedrich A, Tank J, Akahoshi N, Kamata S, Ishii I, Gollasch M, Cystathionine γ-lyase-produced hydrogen sulfide controls endothelial NO bioavailability and blood pressure, Hypertension 71 (6) (2018) 1210–1217. [PubMed: 29712741]

(45). Tao B, Wang R, Sun C, Zhu Y, 3-mercaptopyruvate sulfurtransferase, not cystathionine β-synthase nor cystathionine γ-lyase, mediates hypoxia-induced migration of vascular endothelial cells, Front. Pharmacol 8 (2017) 657. [PubMed: 28979207]

(46). Teng H, Wu B, Zhao K, Yang G, Wu L, Wang R, Oxygen-sensitive mitochondrial accumulation of cystathionine beta-synthase mediated by Lon protease, Proc. Natl. Acad. Sc.i USA 110 (31) (2013)12679–12684.

(47). To-Figueras J, Ozalla D, Mateu CH, Long-standing changes in the urinary profile of porphyrin isomers after clinical remission of porphyria cutanea tarda, Ann. Clin. Lab. Sci 33 (2003) 251–256. [PubMed: 12956438]

(48). Wang CN, Liu YJ, Duan GL, Zhao W, Li XH, Zhu XY, Ni X, CBS and CSE are critical for maintenance of mitochondrial function and glucocorticoid production in adrenal cortex, Antioxid. Redox. Signal 21 (16) (2014) 2192–2207. [PubMed: 24702258]

(49). Wang M, Guo Z, Wang S, Regulation of cystathionine γ-lyase in mammalian cells by hypoxia, Biochem. Genet. 52 (1–2) (2014) 29–37. [PubMed: 23852134]

(50). Wang R, Physiological implications of hydrogen sulfide: a whiff exploration that blossomed, Physiol. Rev. 92 (2) (2012) 791–896. [PubMed: 22535897]

(51). Wang Y, Zhao X, Jin H, Wei H, Li W, Bu D, Tang X, Ren Y, Tang C, Du J, Role of hydrogen sulfide in the development of atherosclerotic lesions in apolipoprotein E knockout mice, Arterioscler. Thromb. Vasc. Biol 29 (2) (2009) 173–179. [PubMed: 18988885]

(52). Wen JY, Gao SS, Chen FL, Chen S, Wang M, Chen ZW, Role of CSE-produced H2S on cerebrovascular relaxation via RhoA-ROCK inhibition and cerebral ischemia-reperfusion injury in mice, ACS Chem. Neurosci 10 (3) (2019) 1565–1574. [PubMed: 30406996]

(53). Yang G, Ju Y, Fu M, Zhang Y, Pei Y, Racine M, Baath S, Merritt TJS, Wang R, Wu L, Cystathionine gamma-lyase/hydrogen sulfide system is essential for adipogenesis and fat mass accumulation in mice, Biochim. Biophys. Acta Mol. Cell Biol. Lipids 1863 (2) (2018) 165–176. [PubMed: 29191638]

(54). Yang G, Wu L, Jiang B, Yang W, Qi J, Cao K, Meng Q, Mustafa AK, Mu W, Zhang S, Snyder SH, Wang R, H_2S as a physiologic vasorelaxant: hypertension in mice with deletion of cystathionine gamma-lyase, Science 322 (5901) (2008) 587–590. [PubMed: 18948540]

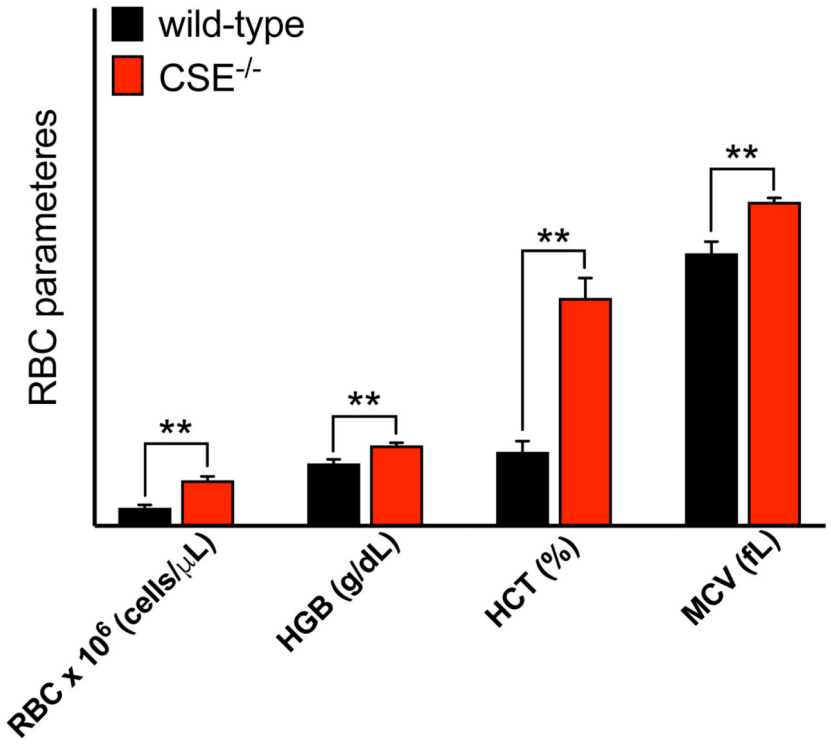

Figure 1: CSE$^{-/-}$ mice exhibit elevated RBC parameters.

Analysis of plasma from CSE$^{-/-}$ mice showed elevated RBC counts, hemoglobin, hematocrit and MCV values compared to wild-type mice. Data are shown as mean ± SEM of CSE$^{-/-}$ (n=13) and wild-type (n=8) mice.

**p<0.01 *vs.* wild-type mice, indicates elevated RBC parameters.

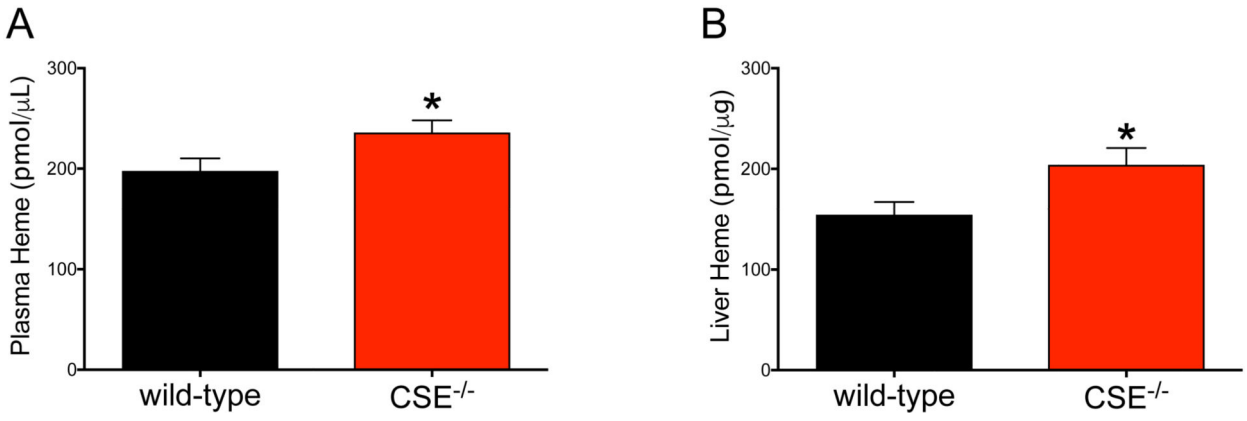

Figure 2: CSE$^{-/-}$ mice show elevated levels of plasma and liver heme.

Increased heme moiety of plasma (1.2 fold) and liver (1.3 fold) proteins of CSE$^{-/-}$ mice were determined by converting heme to the fluorescent protoporphyrin IX. Data are shown as mean ± SEM of CSE$^{-/-}$ and wild-type mice (n>20 animal/group). *p<0.05 compared to the wild-type group shows elevated heme levels.

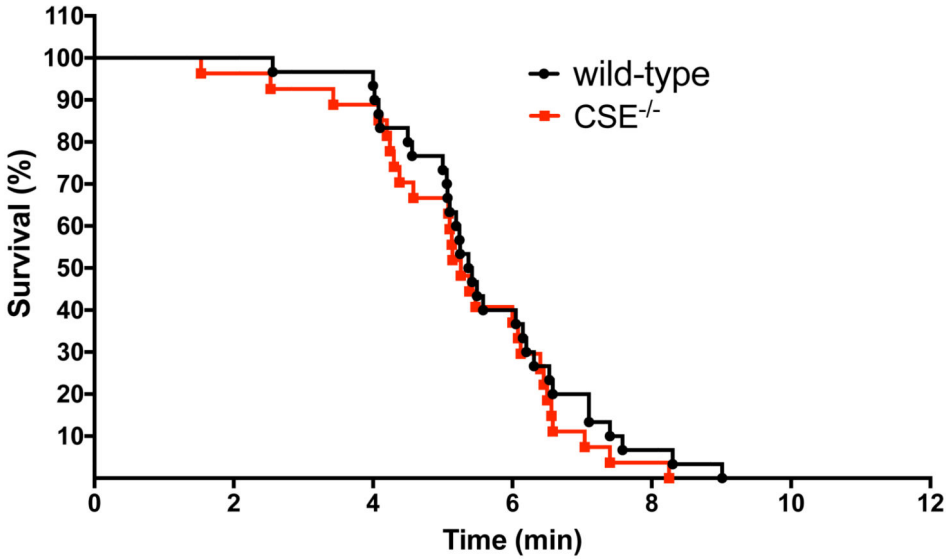

Figure 3. Absence of CSE does not affect survival rate in 5% hypoxia.

$CSE^{-/-}$ and wild-type mice were subjected to 5% hypoxia. Statistical analysis of curve comparisons shows no statistical significance in the short-term survival rate between $CSE^{-/-}$ and wild-type mice (n=27 $CSE^{-/-}$ and n=30 wild-type mice).

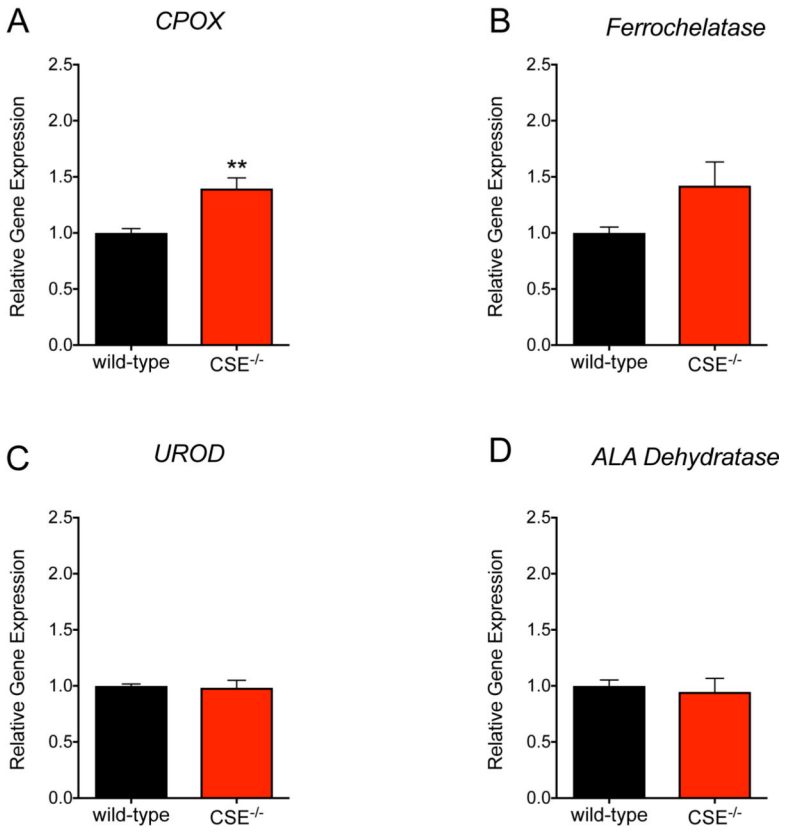

Figure 4. Increased CPOX gene expression in liver tissues of CSE$^{-/-}$ mice.

The mRNA level of CPOX was significantly elevated in liver tissue from CSE$^{-/-}$ *vs.* wild-type mice. The gene expression level of ferrochelatase was also increased but it did not reach statistical significance (p = 0.053). However, the mRNA levels of uroporphyrinogen decarboxylase or ALA dehydratase was not changed. Data are shown as mean ± SEM o CSE $^{-/-}$ and wild-type mice (n=22 animal/group). **p<0.01 *vs.* wild-type group indicates elevated CPOX gene expression.

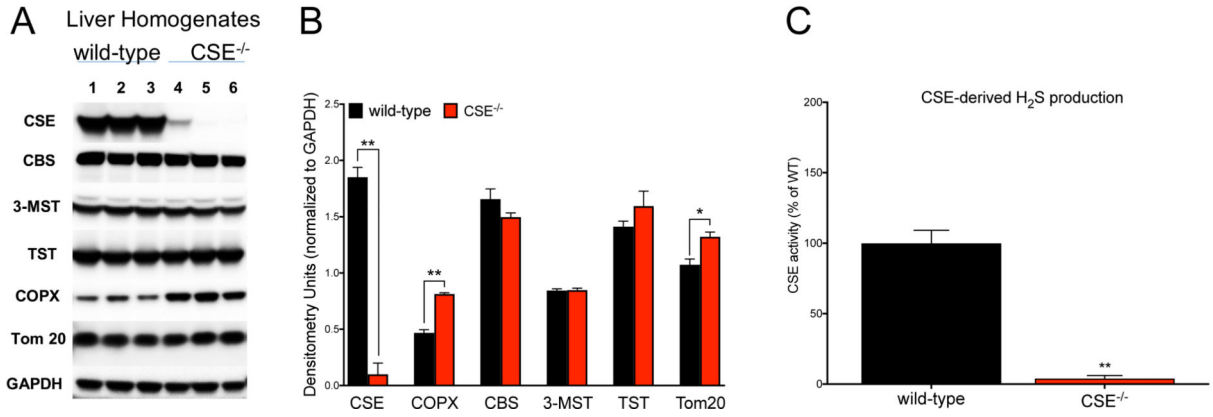

Figure 5. Increased CPOX protein expression in liver tissues of CSE$^{-/-}$ mice.

(**A, B**) Western blot analysis of liver homogenates of CSE$^{-/-}$ *vs.* wild-type mice confirmed (1) lack of CSE, (2) increased CPOX and Tom 20, and (3) no alterations of CBS, 3-MST, and TST protein levels. (**C**) H_2S production by CSE was completely absent in liver tissue homogenates from CSE$^{-/-}$ mice. Data are shown as mean ± SEM of CSE$^{-/-}$ and wild-type mice using n=3 animals/group. *p<0.05, **p<0.01 *vs.* wild-type group.

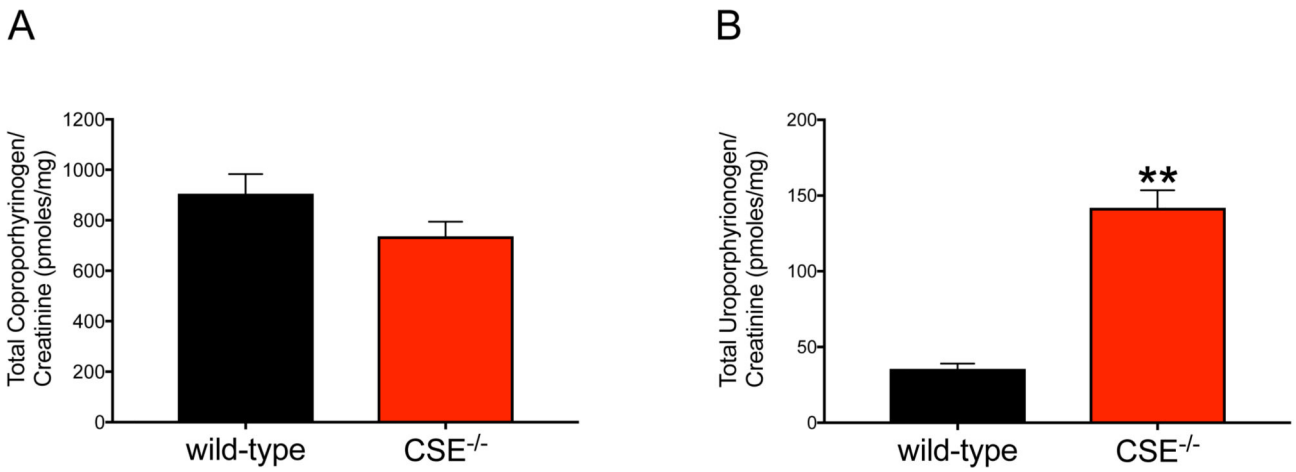

Figure 6: Changes in Coproporphyrinogen and Uroporphyrinogen levels in urine samples from CSE$^{-/-}$ and wild-type mice.

Urine samples from CSE$^{-/-}$ (n=9) and wild-type (n=11) mice were collected using metabolic cages overnight (16 hours). For each sample, creatinine content was determined (Creatinine Colorimetric Assay, BioVision). The measured porphyrins were normalized to urine creatinine for each sample. Data demonstrates reduced tendency of total coproporphyrinogen (**A**) and significantly increased uroporphyrinogen (**B**) in urine samples from CSE$^{-/-}$ mice suggesting upregulated activity of CPOX enzyme. Data are shown as mean ± SEM of coproporphyrinogen and uroporphyrinogen concentrations normalized to urine creatinine content. *p<0.05 *vs.* wild-type group.

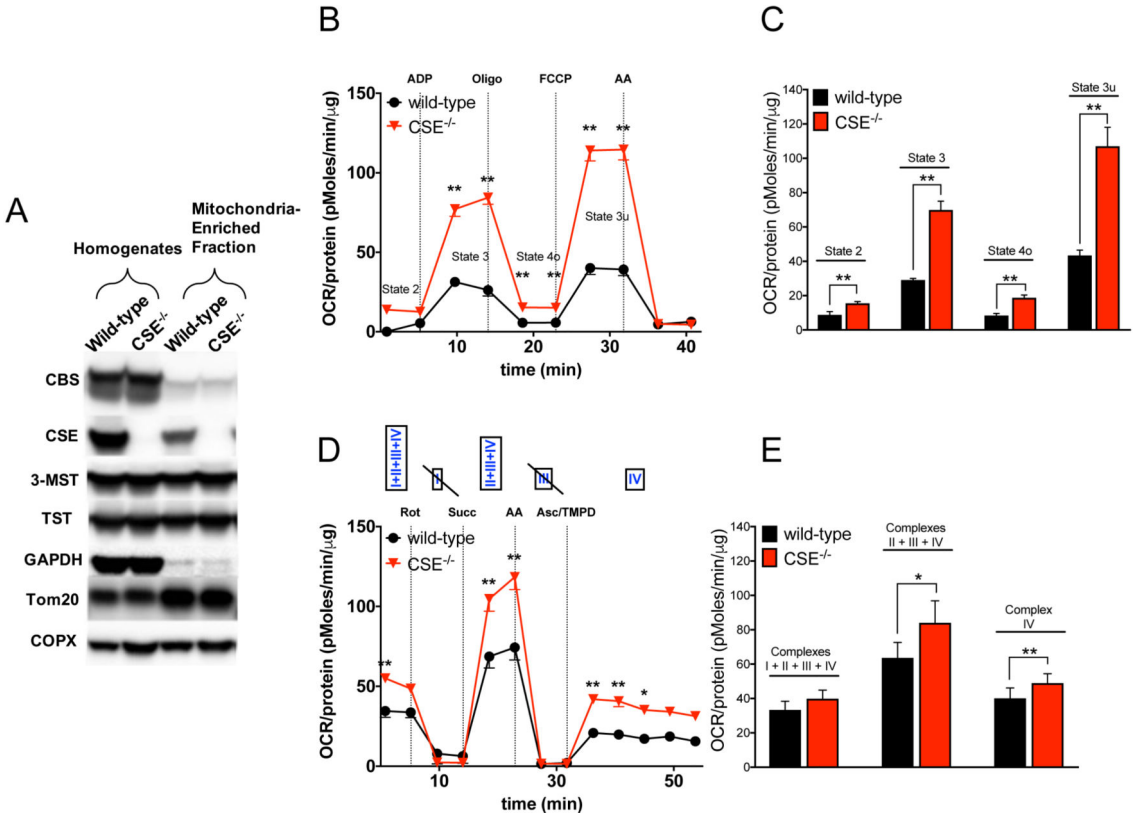

Figure 7. Absence of CSE stimulates mitochondrial respiration in isolated liver mitochondria *ex vivo*.

(**A**) Representative western blot images of mitochondria-enriched fractions using differential centrifugation. CPOX protein expression was significantly higher both liver homogenates and mitochondria-enriched fraction from $CSE^{-/-}$ mice. Tom 20 was higher in $CSE^{-/-}$ liver homogenates and found to be abundant in mitochondria-enriched fractions from both $CSE^{-/-}$ and wild-type mice. CBS was present in both the homogenates and mitochondria-enriched fractions. (**B, C**) Absence of CSE resulted in enhanced mitochondrial oxidative phosphorylation of state 3, 4o and 3u in isolated $CSE^{-/-}$ liver mitochondria compared to wild-type group ('coupling' assay). Figure 7B represents an original tracing of a 'coupling' bioenergetic assay, whereas Figure 7C shows area-under-the-curve (AUC) of key bioenergetic parameters of n=3 independent 'coupling' experiments conducted in liver mitochondria. (**D, E**) Electron flow experiments demonstrated that the absence of CSE exerted stimulatory effects when Complexes I–IV or II–IV or Complex IV alone were functional simultaneously ('electron flow' assays). Figure 7D represents an original tracing of a 'electron flow' bioenergetic assay, whereas Figure 7E shows area-under-the-curve (AUC) of key bioenergetic parameters of n=3 independent 'electron flow' experiments conducted in liver mitochondria. Data are shown as mean ± SEM of $CSE^{-/-}$ and wild-type mice using n=3 animals/group. *p<0.05, **p<0.01 *vs.* wild-type group.

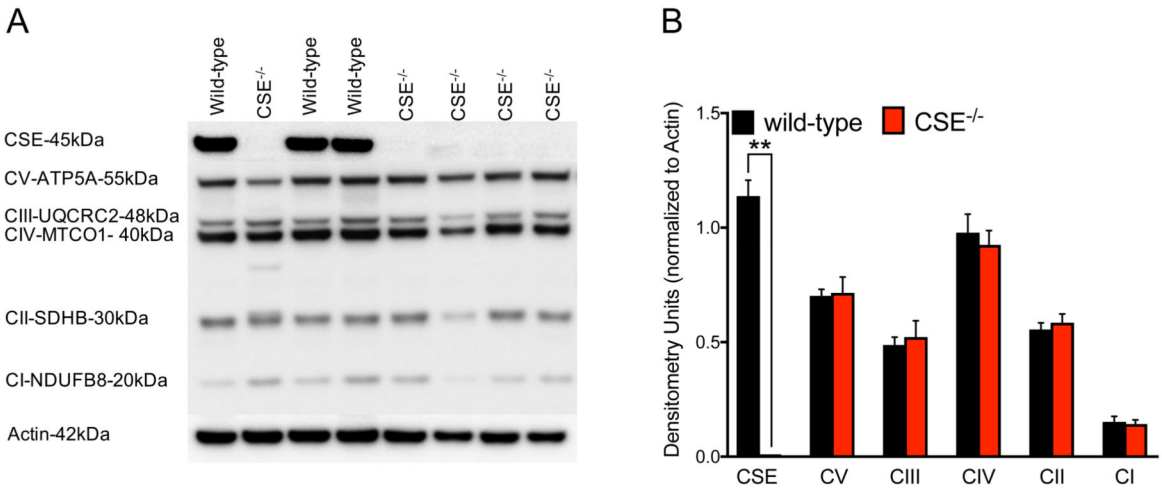

Figure 8. No changes found in the expression levels of mitochondrial complexes.

Western blot analysis determined no differences in protein level of mitochondrial complexes in liver homogenates from $CSE^{-/-}$ mice compared to wild-type. (**A**) Representative Western blot image. (**B**) Densitometry analysis shows as mean ± SEM of $CSE^{-/-}$ (n=11) and wild-type (n=7) mice.

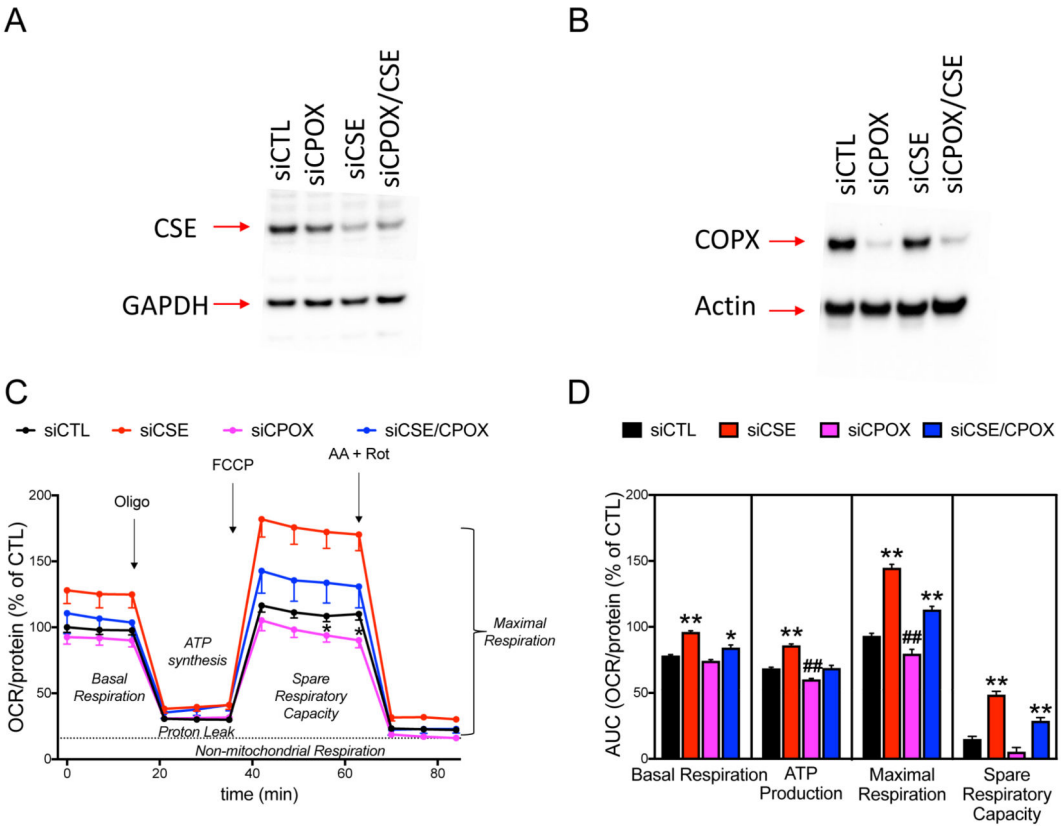

Figure 9. Transient silencing of CSE and CPOX exhibit opposite effects on mitochondrial respiration of cultured liver cells.

Representative Western blot images demonstrate significant attenuation of (**A**) CSE and (**B**) CPOX protein expressions mediated by siRNA silencing approach. (**C**) Mitochondrial respiration of n=3 Seahorse 'coupling' assays. (**D**) Calculated AUC of key bioenergetic parameters such as basal respiration, ATP production, maximal respiration, and spare respiratory capacity. Note that CSE silencing significantly enhanced mitochondrial respiration in all parameters, whereas CPOX silencing worsened the calculated ATP production or maximal respiration values. Double silencing of CSE and CPOX overall improved the basal respiration, ATP production, and maximal respiration compared to vehicle. Data are shown as mean ± SEM of n=3 independent experiments. *p<0.05, **p<0.01 $CSE^{-/-}$ vs. siCTL group or $CSE^{-/-}$/siCPOX vs. siCPOX group; $^{\#}$p<0.05, $^{\#\#}$p<0.01 siCPOX *vs.* siCTL group.

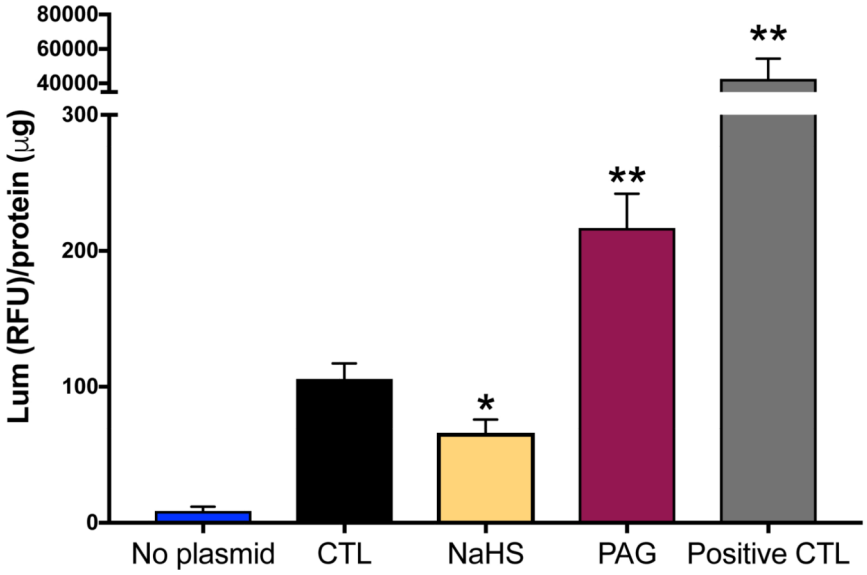

Figure 10. A pharmacological CSE inhibitor increases, while supplementation of exogenous H_2S decreases CPOX promoter activity in cultured liver cells.

A CPOX luciferase reporter construct was established in HepG2 liver cells. Addition of the pharmacological inhibitor of CSE (PAG) or NaHS exerted stimulatory *vs.* inhibitory effects on CPOX promoter/gene activity. In this assay, the negative and postive control vectors were provided and used according to manufacturer's instructions. CTL group showed basic CPOX promoter activity. Data are shown as mean ± SEM of n=6 repeats. *p<0.05, **p<0.01 *vs.* CTL group.

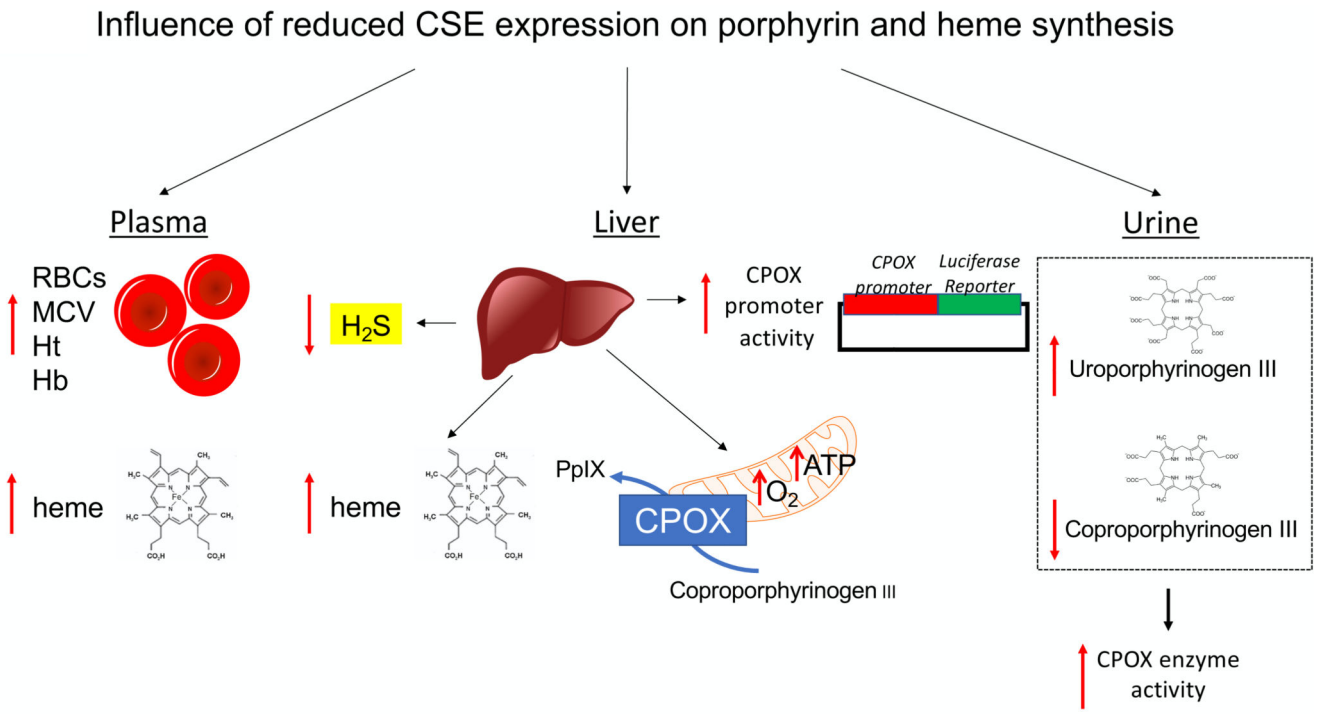

Figure 11. Downregulation of CSE influences porphyrin and heme synthesis.

Ablation of H_2S biosynthesis in the $CSE^{-/-}$ mice or pharmacological inhibition of CSE activity in liver cells yields: (1) elevated red blood cell counts, red blood cell MCVs, hematocrit, hemoglobin and heme levels in plasma samples of $CSE^{-/-}$ mice; (2) reduced CSE-derived H_2S production, increased heme level, CPOX protein expression and mitochondrial function in liver samples of $CSE^{-/-}$ mice; (3) pharmacological inhibition of CSE activity in liver cell cultures increases CPOX gene promoter activity whereas addition of H_2S suppresses it; (4) elevated uroporphyrinogen III and reduced coproporphyrinogen III can be detected in the urine samples of $CSE^{-/-}$ mice, suggestive of increased CPOX enzyme activity. RBC: red blood cell; MCV: mean corpuscular volume; Ht: hematocrit; Hb: hemoglobin; CPOX: Coproporphyrinogen oxidase; PpIX: Protoporphyrin IX.

Table 1:

Real-time PCR primer sequences for gene targets in liver tissues

Genes of interest	Forward primers 5’-3’	Reverse primers 5’-3’
CPOX	ATGCCCTTCTTGGGAACTTT	TAGCCCTGGCTGGACTAGAA
Ferrochelatase	GTGAGCGGGGGAGGAAGAACA	TTGGCTGGTGAAGAAGGATTTAGT
UROD	CCTCTGGATGCTGCCATAAT	TAAGGGTGATGGCTTGGAAC
ALA dehydratase	GGGAGGAGAAAGGGAACAAG	TTTGTTTTGGTGGCTCCTTC
GAPDH	TCACTGCCACCCAGAAGACT	TGAAGTCGCAGGAGACAACC

Table 2:

Gradient elution program with 100 µl injection volume of the urine samples

Step	Time (min)	Flow (ml/min)	Mobile Phase A	Mobile Phase B	Curve
0	2.0	1.20	100	0	0.0
1	2.0	1.20	85	15	6.0
2	25.0	1.20	0	100	2.0
3	7.0	1.20	100	0	2.0

Table 3:

No significant differences in blood gas parameters of $CSE^{-/-}$ and wild-type mice.

Glucose, HCO_3, pO_2, pCO_2, lactate, pH, and total hemoglobin were determined from arterial blood. pO_2, pCO_2, lactate, and pH were measured from venous blood. Data show significant increase in hemoglobin level of $CSE^{-/-}$ mice (13±0.4, n=6) compared to the wild-type group (12±0.4, n=6). No significant differences in lung functions (qs/Qt, PaO_2/FiO_2) were noted between $CSE^{-/-}$ and wild-type mice.

Blood gas parameters	Wild-type			$CSE^{-/-}$			
	Mean	SEM	n	Mean	SEM	n	p value
Arterial blood							
glucose (mg/dL)	206	8	6	182	19	6	0.29
HCO3 (mmol/L)	18,0	0,4	6	18,1	1,1	6	0.93
pO2 (mmHg)	116,6	3,5	6	109,9	8,5	6	0.48
pCO2 (mmHg)	29,6	1,3	6	29,3	1,6	6	0.89
lactate (mmol/L)	3,0	0,3	6	2,7	0,2	6	0.54
pH	7,39	0,02	6	7,40	0,0	6	0.86
total Hb (g/dL)	12,5	0	6	13,5	0,3	6	0.043 *
Venous blood							
pO2 (mmHg)	42,7	3,7	6	39,5	2,4	6	0.48
pCO2 (mmHg)	33,3	0,9	6	33,5	3,9	6	0.95
lactate (mmol/L)	3,1	0,3	6	3,4	0,5	6	0.68
pH	7,35	0,01	6	7,34	0,03	6	0.63
Shunt fraction							
qs/Qt	0,074	0,014	6	0,072	0,011	6	0.95
PaO2/FiO2	555,6	16,9	6	523,7	40,74	6	0.48

* $p<0.05$ *vs.* wild-type group.

Table 4:

Changes in porphyrin concentrations in urine samples from CSE KO and wild-type mice.

Urine samples from $CSE^{-/-}$ (n = 9) and wild-type (n = 11) mice were collected using metabolic cages overnight (16 hours). For each sample, creatinine content was determined (Creatinine Colorimetric Assay, BioVision) and porphyrins were measured by HPLC. Among all the porphyrin derivates, coproporphyrinogen (coproporphyrinogen I and III are two metabolic isomers of coproporphyrinogen) and uroporphyrinogen (uroporphyrinogen I and III are two metabolic isomers of uroporphyrinogen) were significantly detectable. Data show decreased tendency of coproporphyrinogen and significantly increased level of uroporphyrinogen in urine samples from $CSE^{-/-}$ mice indicating upregulated activity of CPOX enzyme. Data are shown as mean ± SEM of porphyrin concentrations normalized to urine creatinine content of each $CSE^{-/-}$ and wild-type mice.

8-COOH, Porphyrin Octacarboxcylic Acid/Uroporphyrinogen											p value *vs.* WT mice
Group #	**# of mice/ group**	**Porphyrin**	**Porphyrin (%)**	**Total urine volume (mL)**	**Creatinine (mg/100 mL)**	**Porphyrin/ 100μL urine (pmoles/ 100μL)**	**Porphyrin/ mL urine (pmoles/mL)**	**Porphyrin/ Total urine volume (pmoles/mL)**	**Total urine creatinine (mg)**	**Porphyrin/ Total urine creatinine (pmoles/mg)**	***vs.* Total porphrins**
CSE KO # 1	2 ♂	Uro Total	2.95	1.50	13.42	2.21	22.10	33.15	0.20	164.64	*p<0,0001
		Uro I	2.04			1.53	15.30	22.95		113.98	
		Uro III	0.91			0.68	6.80	10.20		50.66	
CSE KO # 2	2 ♂	Uro Total	3.11	2.00	13.65	2.14	21.40	42.80	0.27	156.81	
		Uro I	1.94			1.34	13.40	26.80		98.19	
		Uro III	1.17			0.80	8.00	16.00		58.62	
CSE KO # 3	2 ♂	Uro Total	3.15	1.20	17.03	1.95	19.50	23.40	0.20	114.52	
		Uro I	2.05			1.71	17.10	20.52		100.43	
		Uro III	1.10			0.24	2.40	2.88		14.10	
CSE KO # 4	3 ♂	Uro Total	2.83	4.30	12.89	1.70	17.00	73.10	0.55	131.84	
		Uro I	1.86			1.12	11.20	48.16		86.86	
		Uro III	0.97			0.58	5.80	24.94		44.98	

7-COOH, Porphyrin Heptacarboxcylic Acid											p value *vs.* WT mice
Group #	**# of mice/ group**	**Porphyrin**	**Porphyrin (%)**	**Total urine volume (mL)**	**Creatinine (mg/100 mL)**	**Porphyrin/ 100μL urine (pmoles/ 100μL)**	**Porphyrin/ mL urine (pmoles/mL)**	**Porphyrin/ Total urine volume (pmoles/mL)**	**Total urine creatinine (mg)**	**Porphyrin/ Total urine creatinine (pmoles/mg)**	***vs.* Total porphrins**

CSE KO # 1	2 ♂	7 COOH Total	0.14	1.50	13.42	0.10	1.01	1.52	0.20	7.52	p=0,4169
		7 COOH-I	0.04			0.03	0.32	0.48		2.38	
		7 COOH-III	0.10			0.07	0.69	1.04		5.14	
CSE KO # 2	2 ♂	7 COOH Total	0.08	2.00	13.65	0.06	0.57	1.14	0.27	4.18	
		7 COOH-I	0.02			0.01	0.13	0.26		0.95	
		7 COOH-III	0.06			0.04	0.44	0.88		3.22	
CSE KO # 3	2 ♂	7 COOH Total	0.11	1.20	17.03	0.06	0.58	0.70	0.20	3.41	
		7 COOH-I	0.00			0.00	0.00	0.00		0.00	
		7 COOH-III	0.11			0.06	0.58	0.70		3.41	
CSE KO # 4	3 ♂	7 COOH Total	0.15	4.30	12.89	0.09	0.88	3.78	0.55	6.82	
		7 COOH-I	0.00			0.00	0.00	0.00		0.00	
		7 COOH-III	0.15			0.09	0.88	3.78		6.82	

6-COOH, Porphyrin Hexacarboxcylic Acid

Group #	# of mice/ group	Porphyrin	Porphyrin (%)	Total urine volume (mL)	Creatinine (mg/100 mL)	Porphyrin/ 100µL urine (pmoles/ 100µL)	Porphyrin/ mL urine (pmoles/mL)	Porphyrin/ Total urine volume (pmoles/mL)	Total urine creatinine (mg)	Porphyrin/ Total urine creatinine (pmoles/mg)	p value *vs.* WT mice *vs.* Total porphrins
CSE KO # 1	2 ♂	6 COOH Total	0.06	1.50	13.42	0.05	0.49	0.74	0.20	3.65	*p<0,0001
		6 COOH-I	0.03			0.02	0.23	0.35		1.71	
		6 COOH-III	0.03			0.03	0.26	0.39		1.94	
CSE KO # 2	2 ♂	6 COOH Total	0.05	2.00	13.65	0.05	0.49	0.98	0.27	3.59	
		6 COOH-I	0.00			0.00	0.23	0.46		1.69	
		6 COOH-III	0.05			0.05	0.26	0.52		1.91	
CSE KO # 3	2 ♂	6 COOH Total	0.01	1.20	17.03	0.01	0.49	0.59	0.20	2.88	
		6 COOH-I	0.00			0.00	0.23	0.28		1.35	
		6 COOH-III	0.01			0.01	0.26	0.31		1.53	

CSE KO # 4	3 ♂	6 COOH Total	0.00	4.30	12.89	0.00	0.49	2.11	0.55	3.80	
		6 COOH-I	0.00			0.00	0.23	0.99		1.78	
		6 COOH-III	0.00			0.00	0.26	1.12		2.02	

5-COOH, Porphyrin Pentacarboxcylic Acid											p value *vs.* WT mice
Group #	**# of mice/ group**	**Porphyrin**	**Porphyrin (%)**	**Total urine volume (mL)**	**Creatinine (mg/100 mL)**	**Porphyrin/ 100μL urine (pmoles/ 100μL)**	**Porphyrin/ mL urine (pmoles/mL)**	**Porphyrin/ Total urine volume (pmoles/mL)**	**Total urine creatinine (mg)**	**Porphyrin/ Total urine creatinine (pmoles/mg)**	***vs.* Total porphrins**
CSE KO # 1	2 ♂	5 COOH Total	3.05	1.50	13.42	2.30	23.00	34.50	0.20	171.35	p=0,1761
		5 COOH-I	0.94			0.71	7.10	10.65		52.89	
		5 COOH-III	2.11			1.59	15.90	23.85		118.45	
CSE KO # 2	2 ♂	5 COOH Total	1.53	2.00	13.65	1.18	11.80	23.60	0.27	86.46	
		5 COOH-I	0.17			0.13	1.30	2.60		9.53	
		5 COOH-III	1.36			1.05	10.50	21.00		76.94	
CSE KO # 3	2 ♂	5 COOH Total	1.58	1.20	17.03	1.34	13.40	16.08	0.20	78.70	
		5 COOH-I	0.14			0.12	1.20	1.44		7.05	
		5 COOH-III	1.44			1.22	12.20	14.64		71.65	
CSE KO # 4	3 ♂	5 COOH Total	0.72	4.30	12.89	1.34	13.40	57.62	0.55	103.92	
		5 COOH-I	0.10			0.05	0.54	2.32		4.19	
		5 COOH-III	0.62			0.37	3.70	15.91		28.69	

4-COOH, Porphyrin Tetracarboxylic Acid/Coproporphyrinogen											p value *vs.* WT mice
Group #	**# of mice/ group**	**Porphyrin**	**Porphyrin (%)**	**Total urine volume (mL)**	**Creatinine (mg/100 mL)**	**Porphyrin/ 100μL urine (pmoles/ 100μL)**	**Porphyrin/ mL urine (pmoles/mL)**	**Porphyrin/ Total urine volume (pmoles/mL)**	**Total urine creatinine (mg)**	**Porphyrin/ Total urine creatinine (pmoles/mg)**	***vs.* Total porphrins**
CSE KO # 1	2 ♂	Copro Total	14.28	1.50	13.42	10.74	107.40	161.10	0.20	800.12	p=0,1397
		Copro I	1.49			1.12	11.20	16.80		83.44	
		Copro III	12.79			9.62	96.20	144.30		716.68	

CSE KO # 2	2 ♂	Copro Total	14.17	2.00	13.65	10.51	105.10	210.20	0.27	770.11
		Copro I	0.89			0.66	6.60	13.20		48.36
		Copro III	13.28			9.85	98.50	197.00		721.75
CSE KO # 3	2 ♂	Copro Total	16.73	1.20	17.03	13.81	138.10	165.72	0.20	811.05
		Copro I	0.98			0.81	8.10	9.72		47.57
		Copro III	15.75			13.00	130.00	156.00		763.48
CSE KO # 4	3 ♂	Copro Total	12.19	4.30	12.89	7.30	73.00	313.90	0.55	566.13
		Copro I	0.51			0.31	3.10	13.33		24.04
		Copro III	11.68			6.99	69.90	300.57		542.09

8-COOH, Porphyrin Octacarboxcylic Acid/Uroporphyrinogen

Group #	# of mice/ group	Porphyrin	Porphyrin (%)	Total urine volume (mL)	Creatinine (mg/100 mL)	Porphyrin/ 100µL urine (pmoles/ 100µL)	Porphyrin/ mL urine (pmoles/mL)	Porphyrin/ Total urine volume (pmoles/mL)	Total urine creatinine (mg)	Porphyrin/ Total urine creatinine (pmoles/mg)
WT # 1	2 ♂	Uro Total	1.13	1.90	19.14	0.61	6.10	11.59	0.36	31.87
		Uro I	1.13			0.61	6.10	11.59		31.87
		Uro III	0.00			0.00	0.00	0.00		0.00
WT # 2	3 ♂	Uro Total	0.95	4.10	13.02	0.48	4.80	19.68	0.53	36.86
		Uro I	0.91			0.46	4.60	18.86		35.32
		Uro III	0.04			0.02	0.20	0.82		1.54
WT # 3	2 ♂	Uro Total	0.54	3.80	10.35	0.25	2.52	9.58	0.39	24.35
		Uro I	0.16			0.08	0.76	2.89		7.34
		Uro III	0.38			0.18	1.76	6.69		17.01
WT # 4	2 ♂	Uro Total	1.05	1.90	13.90	0.56	5.63	10.70	0.26	40.49
		Uro I	0.90			0.48	4.81	9.14		34.60
		Uro III	0.15			0.08	0.82	1.56		5.90
WT # 5	2 ♂	Uro Total	1.20	3.40	11.08	0.49	4.94	16.81	0.38	44.59
		Uro I	1.08			0.45	4.46	15.16		40.24
		Uro III	0.12			0.05	0.48	1.64		4.36

7-COOH, Porphyrin Heptacarboxcylic Acid

Group #	# of mice/ group	Porphyrin	Porphyrin (%)	Total urine volume (mL)	Creatinine (mg/100 mL)	Porphyrin/ 100µL urine (pmoles/ 100µL)	Porphyrin/ mL urine (pmoles/mL)	Porphyrin/ Total urine volume	Total urine creatinine (mg)	Porphyrin/ Total urine creatinine (pmoles/mg)

								(pmoles/mL)		
WT # 1	2 ♂	7 COOH Total	0.12	1.90	19.14	0.06	0.61	1.16	0.36	3.19
		7 COOH-I	0.00			0.00	0.00	0.00		0.00
		7 COOH-III	0.12			0.06	0.61	1.16		3.19
WT # 2	3 ♂	7 COOH Total	0.07	4.10	13.02	0.04	0.37	1.52	0.53	2.84
		7 COOH-I	0.00			0.00	0.00	0.00		0.00
		7 COOH-III	0.07			0.04	0.37	1.52		2.84
WT # 3	2 ♂	7 COOH Total	0.15	3.80	10.35	0.07	0.69	2.64	0.39	6.71
		7 COOH-I	0.00			0.00	0.00	0.00		0.00
		7 COOH-III	0.15			0.07	0.69	2.64		6.71
WT # 4	2 ♂	7 COOH Total	0.02	1.90	13.90	0.01	0.12	0.23	0.26	0.86
		7 COOH-I	0.00			0.00	0.00	0.00		0.00
		7 COOH-III	0.02			0.01	0.12	0.23		0.86
WT # 5	2 ♂	7 COOH Total	0.18	3.40	11.08	0.08	0.77	2.61	0.38	6.93
		7 COOH-I	0.01			0.01	0.08	0.26		0.68
		7 COOH-III	0.17			0.07	0.69	2.35		6.25

6-COOH, Porphyrin Hexacarboxcylic Acid

Group #	# of mice/ group	Porphyrin	Porphyrin (%)	Total urine volume (mL)	Creatinine (mg/100 mL)	Porphyrin/ 100μL urine (pmoles/ 100μL)	Porphyrin/ mL urine (pmoles/mL)	Porphyrin/ Total urine volume (pmoles/mL)	Total urine creatinine (mg)	Porphyrin/ Total urine creatinine (pmoles/mg)
WT # 1	2 ♂	6 COOH Total	0.03	1.90	19.14	0.01	0.13	0.25	0.36	0.68
		6 COOH-I	0.00			0.00	0.00	0.00		0.00
		6 COOH-III	0.03			0.01	0.13	0.25		0.68
WT # 2	3 ♂	6 COOH Total	0.00	4.10	13.02	0.00	0.00	0.00	0.53	0.00
		6 COOH-I	0.00			0.00	0.00	0.00		0.00
		6 COOH-III	0.00			0.00	0.00	0.00		0.00
WT # 3	2 ♂	6 COOH Total	0.01	3.80	10.35	0.01	0.06	0.23	0.39	0.58
		6 COOH-I	0.00			0.00	0.00	0.00		0.00
		6 COOH-III	0.01			0.01	0.06	0.23		0.58

WT # 4	2 ♂	6 COOH Total	0.01	1.90	13.90	0.01	0.11	0.21	0.26	0.79
		6 COOH-I	0.00			0.00	0.00	0.00		0.00
		6 COOH-III	0.01			0.01	0.11	0.21		0.79
WT # 5	2 ♂	6 COOH Total	0.00	3.40	11.08	0.00	0.00	0.00	0.38	0.00
		6 COOH-I	0.00			0.00	0.00	0.00		0.00
		6 COOH-III	0.00			0.00	0.00	0.00		0.00

5-COOH, Porphyrin Pentacarboxcylic Acid

Group #	# of mice/ group	Porphyrin	Porphyrin (%)	Total urine volume (mL)	Creatinine (mg/100 mL)	Porphyrin/ 100μL urine (pmoles/ 100μL)	Porphyrin/ mL urine (pmoles/mL)	Porphyrin/ Total urine volume (pmoles/mL)	Total urine creatinine (mg)	Porphyrin/ Total urine creatinine (pmoles/mg)
WT # 1	2 ♂	5 COOH Total	0.85	1.90	19.14	0.45	4.54	8.63	0.36	23.72
		5 COOH-I	0.08			0.04	0.44	0.84		2.30
		5 COOH-III	0.77			0.41	4.10	7.79		21.42
WT # 2	3 ♂	5 COOH Total	1.94	4.10	13.02	0.98	9.84	40.34	0.53	75.56
		5 COOH-I	0.06			0.03	0.30	1.23		2.30
		5 COOH-III	1.88			0.95	9.54	39.11		73.26
WT # 3	2 ♂	5 COOH Total	3.08	3.80	10.35	1.44	14.36	54.57	0.39	138.77
		5 COOH-I	0.29			0.13	1.33	5.05		12.85
		5 COOH-III	2.79			1.30	13.03	49.51		125.92
WT # 4	2 ♂	5 COOH Total	1.61	1.90	13.90	0.86	8.62	16.38	0.26	62.00
		5 COOH-I	0.18			0.10	0.98	1.86		7.05
		5 COOH-III	1.43			0.76	7.64	14.52		54.95
WT # 5	2 ♂	5 COOH Total	0.44	3.40	11.08	0.21	2.14	7.28	0.38	19.32
		5 COOH-I	0.05			0.05	0.53	1.82		4.82
		5 COOH-III	0.39			0.16	1.61	5.46		14.50

4-COOH, Porphyrin Tetracarboxylic Acid/Coproporphyrinogen

Group #	# of mice/ group	Porphyrin	Porphyrin (%)	Total urine volume (mL)	Creatinine (mg/100 mL)	Porphyrin/ 100μL urine (pmoles/ 100μL)	Porphyrin/ mL urine (pmoles/mL)	Porphyrin/ Total urine volume (pmoles/mL)	Total urine creatinine (mg)	Porphyrin/ Total urine creatinine (pmoles/mg)

WT # 1	2 ♂	Copro Total	13.65	1.90	19.14	14.72	147.16	279.60	0.36	768.78
		Copro I	0.37			0.40	3.96	7.52		20.69
		Copro III	13.28			14.32	143.20	272.08		748.09
WT # 2	3 ♂	Copro Total	23.03	4.10	13.02	11.72	117.15	480.32	0.53	899.56
		Copro I	0.51			0.26	2.62	10.74		20.12
		Copro III	22.52			11.45	114.53	469.57		879.44
WT # 3	2 ♂	Copro Total	24.70	3.80	10.35	12.45	124.53	473.21	0.39	1203.42
		Copro I	1.36			0.63	6.33	24.05		61.17
		Copro III	23.34			11.82	118.20	449.16		1142.25
WT # 4	2 ♂	Copro Total	21.91	1.90	13.90	11.68	116.78	221.88	0.26	839.92
		Copro I	0.61			0.33	3.26	6.19		23.45
		Copro III	21.30			11.35	113.52	215.69		816.47
WT # 5	2 ♂	Copro Total	21.94	3.40	11.08	9.05	90.45	307.53	0.38	816.00
		Copro I	0.53			0.22	2.20	7.48		19.85
		Copro III	21.41			8.83	88.25	300.05		796.15

* $p \leq 0.05$ *vs.* wild-type group.